

# On the Application of the Asymptotic Method of Global Instability in Aeroelasticity Problems

V. V. Vedeneev<sup>a</sup>

Received July 6, 2016

**Abstract**—The asymptotic method of global instability developed by A.G. Kulikovskii is an effective tool for determining the eigenfrequencies and stability boundary of one-dimensional or multidimensional systems of sufficiently large finite length. The effectiveness of the method was demonstrated on a number of one-dimensional problems; and since the mid-2000s, this method has been used in aeroelasticity problems, which are not strictly one-dimensional: such is only the elastic part of the problem, while the gas flow occupies an unbounded domain. In the present study, the eigenfrequencies and stability boundaries predicted by the method of global instability are compared with the results of direct calculation of the spectra of the corresponding problems. The size of systems is determined starting from which the method makes a quantitatively correct prediction for the stability boundary.

**DOI:** 10.1134/S0081543816080174

## 1. INTRODUCTION

In many problems, one studies the stability of systems whose length in one direction is much greater than in other directions. Examples are given by the stability of boundary layers on solids, flows in pipes, hydro- and aeroelastic stability of thin-walled structures in a fluid flow, and other systems. After linearization of the system of equations for perturbations, one usually analyzes the behavior of solutions of the form  $e^{i(kx-\omega t)}$ , i.e., traveling waves, which in the vast majority of problems completely determine the stability of arbitrary perturbations of an infinitely long system.

However, in finite, albeit arbitrarily long, systems, solutions in the form of a single traveling wave cannot exist, because the waves are reflected from the boundaries even if the latter are far enough from the point where perturbations arise. The stability problem of long but finite systems was solved by Kulikovskii in the general form for one-dimensional [7] (see also [12, § 65]) and multidimensional [10] systems. The main results are as follows:

- even for a system of very large length  $L$ , its stability criterion does not coincide with the stability criterion of an infinitely long system;
- growing perturbations can take either the form of “one-sided” eigenfunctions, which are determined by the reflection of waves from one end, or the form of “global” eigenfunctions, which represent two waves that travel in opposite directions and turn into each other when reflected from the ends of the system;
- if the length  $L$  of the system is large enough, then the growth or damping of one-sided eigenfunctions is determined only by the boundary conditions at the end from which the waves are reflected; the stability criterion of global eigenfunctions does not depend on the specific form of the boundary conditions defined at the ends.

If the instability of a system is determined by the growth of one-sided eigenfunctions, it can generally be eliminated by a change of the physical system such that the boundary condition at

---

<sup>a</sup> Steklov Mathematical Institute of Russian Academy of Sciences, ul. Gubkina 8, Moscow, 119991 Russia.

E-mail address: vasily@vedeneev.ru

the end is changed appropriately. On the contrary, the global instability is determined only by the properties of the system itself and cannot be eliminated by changing the boundary conditions.

The criterion of global instability has been successfully used in the stability analysis of a wide variety of processes: Poiseuille flows in a pipe of finite length [1, 8, 9], thermocapillary convection [16], jet flows of a liquid [19, 32], elastic plates in a flow of an incompressible fluid [15], spiral waves [5], flames [14], and axisymmetric Couette flows of a magnetic fluid [17]. This criterion has also been used in the analysis of some thermoplasticity models [6], in the study of vibrations of fluid-conveying pipes [3, 11], in the study of flutter of panels of flying vehicles in a supersonic gas flow [21, 23, 29, 30], in the analysis of eigenmodes of flows over cavities [20], and in the study of other problems [4].

Although most of these problems are essentially one-dimensional, in the stability problems of plates in a gas flow only a plate is finite, while the region of gas flow is infinite. Such a system is not completely one-dimensional; therefore, analyzing only one-dimensional waves, one cannot obtain an estimate for the size of plates to which an asymptotic method applies. The goal of the present study is to compare the results obtained by the global instability criterion with the results of numerical solution of the flutter problem for an elastic plate in a gas flow and to determine the size of the plate starting from which the asymptotic criterion gives satisfactory results. This issue is important because the asymptotic method provides a quantitatively correct description of both linear and nonlinear [18, 24, 28] phenomena in plane problems, but the effectiveness of the method in three-dimensional problems has not yet been determined.

## 2. STATEMENT OF THE PROBLEM

Consider an elastic plate of finite size built-in into an absolutely rigid plane. On one side of the plate, there is a supersonic gas flow, and on the other side, constant pressure equal to the unperturbed pressure in the flow is maintained, which results in a flat equilibrium state of the plate (Fig. 1). We consider three configurations: a plate in the form of a strip (Fig. 1a), which yields a two-dimensional problem; an infinite series of linked plates of size  $L_{wx} \times L_{wy}$  or, which is the same, a plate in the form of a periodically pinned strip (Fig. 1b); and an isolated plate of size  $L_{wx} \times L_{wy}$  (Fig. 1c). The two-dimensional case reduces to the other cases for  $L_{wy} = \infty$ .

The motion of a plate is described by the Kirchhoff–Love model. The stiffness of the plate is  $D_w$ , its thickness is  $h$ , and the density of its material is  $\rho_m$ . An isotropic in-plane tension force  $N_w = \sigma h$  acts in the plane of the plate, where  $\sigma$  is the tension stress. The gas is assumed to be inviscid and ideal, and the motion is adiabatic. The gas velocity is  $U$ , density is  $\rho$ , and the speed of sound is  $a$ .

In order to pass to dimensionless variables, we take  $a$ ,  $\rho_m$ , and  $h$  as quantities with independent dimensions. Then the dimensionless parameters are expressed in terms of dimensional ones as follows:

$$D = \frac{D_w}{a^2 \rho_m h^3}, \quad M_w = \sqrt{\frac{N_w}{a^2 \rho_m h}}, \quad L_x = \frac{L_{wx}}{h}, \quad L_y = \frac{L_{wy}}{h}, \quad M = \frac{U}{a}, \quad \mu = \frac{\rho}{\rho_m}. \quad (2.1)$$

Here  $D$ ,  $L_x$ , and  $L_y$  are the dimensionless stiffness, length, and width of the plate,  $M$  and  $\mu$  are the Mach number and the dimensionless gas density. The parameter  $M_w$ , which characterizes tension, has the meaning of the dimensionless velocity of long waves in the plate in vacuum.

The Kirchhoff–Love equation of motion of a thin elastic plate in a gas flow and the pinning boundary condition at its edges are expressed in the dimensionless form as follows:

$$\begin{aligned} \frac{\partial^2 w}{\partial t^2} + D \Delta^2 w - M_w^2 \Delta w + p &= 0, & (x, y) \in S, \\ w = \frac{\partial^2 w}{\partial x^2} = 0, \quad x = 0, L_x, \quad w = \frac{\partial^2 w}{\partial y^2} = 0, \quad y = 0, L_y, \end{aligned} \quad (2.2)$$

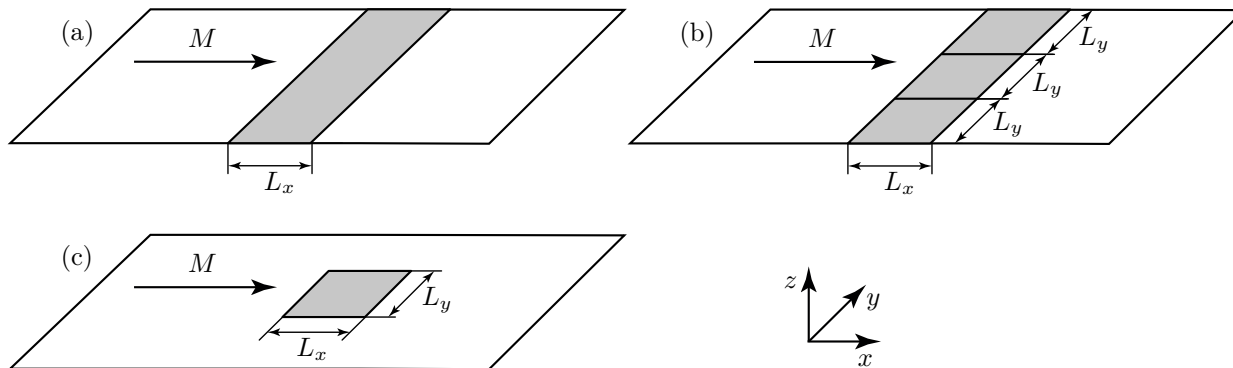


**Fig. 1.** Plate in a gas flow: (a) plate in the form of a strip, (b) series of linked simply supported plates, and (c) an isolated rectangular plate.

where  $w(x, y, t)$  is the plate deflection,  $\Delta$  is the two-dimensional Laplace operator, and  $S = (0, L_x) \times (0, L_y)$  is the surface of the plate. The linearized theory of gas flow implies the following expression for the difference of pressures  $p(x, y, t)$  acting on the plate in terms of the gas-flow potential  $\varphi(x, y, z, t)$ :

$$p(x, y, t) = -\mu \left( \frac{\partial}{\partial t} + M \frac{\partial}{\partial x} \right) \varphi(x, y, 0, t). \tag{2.3}$$

The system of linearized equations and boundary conditions describing small perturbations of gas has the form

$$\begin{aligned} & \left( \frac{\partial}{\partial t} + M \frac{\partial}{\partial x} \right)^2 \varphi - \frac{\partial^2 \varphi}{\partial x^2} - \frac{\partial^2 \varphi}{\partial y^2} - \frac{\partial^2 \varphi}{\partial z^2} = 0, \quad z > 0, \\ & \left( \frac{\partial \varphi}{\partial x}, \frac{\partial \varphi}{\partial y}, \frac{\partial \varphi}{\partial z} \right) \rightarrow 0 \quad \text{as } z \rightarrow +\infty \quad \text{along the characteristics } z = \frac{x - x_0}{\sqrt{M^2 - 1}}, \\ & \frac{\partial \varphi}{\partial z} = \frac{\partial w}{\partial t} + M \frac{\partial w}{\partial x}, \quad z = 0, \quad (x, y) \in S, \quad \frac{\partial \varphi}{\partial z} = 0, \quad z = 0, \quad (x, y) \notin S. \end{aligned} \tag{2.4}$$

Here the first equation is the wave equation in the coordinate system moving at the flow velocity. The second (radiation) condition is imposed only on growing perturbations. The third condition in (2.4) expresses the impermeability of the gas through the oscillating plate and the surrounding absolutely rigid surface.

The stability of an elastic plate in a gas flow is determined by the behavior of eigenmodes; therefore, henceforth we assume that small perturbations of the plate deflection and the potential of the gas flow have the form

$$w(x, y, t) = W(x, y)e^{-i\omega t}, \quad \varphi(x, y, z, t) = \Phi(x, y, z)e^{-i\omega t}. \tag{2.5}$$

Substituting these expressions into the equations for perturbations yields an equation for the eigenmodes of the plate oscillations

$$\begin{aligned} & D \Delta^2 W - M_w^2 \Delta w - \omega^2 W - \mu \left( -i\omega + M \frac{\partial}{\partial x} \right) \Phi(x, y, 0) = 0, \quad (x, y) \in S, \\ & W = \frac{\partial^2 W}{\partial x^2} = 0, \quad x = 0, L_x, \quad W = \frac{\partial^2 W}{\partial y^2} = 0, \quad y = 0, L_y, \end{aligned} \tag{2.6}$$

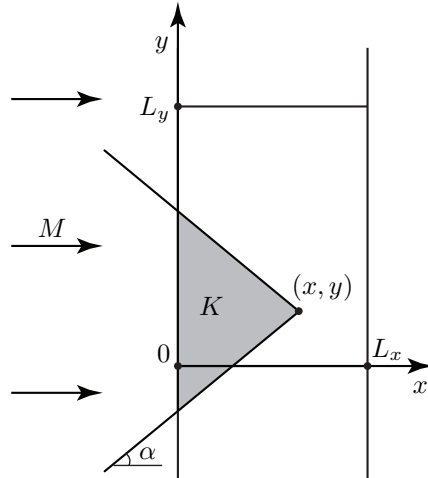


**Fig. 2.** Intersection of the inverse Mach cone emanating from point  $(x, y)$  with the surface of the plate.

and the gas-flow equations

$$\begin{aligned} & \left(-i\omega + M \frac{\partial}{\partial x}\right)^2 \Phi - \frac{\partial^2 \Phi}{\partial x^2} - \frac{\partial^2 \Phi}{\partial y^2} - \frac{\partial^2 \Phi}{\partial z^2} = 0, \quad z > 0, \\ & \left(\frac{\partial \Phi}{\partial x}, \frac{\partial \Phi}{\partial y}, \frac{\partial \Phi}{\partial z}\right) \rightarrow 0 \quad \text{as } z \rightarrow +\infty \quad \text{along the characteristics } z = \frac{x - x_0}{\sqrt{M^2 - 1}}, \quad (2.7) \\ & \frac{\partial \Phi}{\partial z} = -i\omega W + M \frac{\partial W}{\partial x}, \quad z = 0, \quad (x, y) \in S, \quad \frac{\partial \Phi}{\partial z} = 0, \quad z = 0, \quad (x, y) \notin S. \end{aligned}$$

The equation for the potential  $\Phi$  with boundary conditions (2.7) is solved analytically using the Laplace transform [13, §4.8]. On the surface of the plate, the solution is given by

$$\begin{aligned} \Phi(x, y, 0) = & -\frac{1}{\pi} \iint_K \left(-i\omega W(x_1, y_1) + M \frac{\partial W(x_1, y_1)}{\partial x_1}\right) \exp\left(\frac{i\omega M}{\beta^2} (x - x_1)\right) \\ & \times \frac{1}{\sqrt{(x - x_1)^2 - \beta^2 y_1^2}} \cos\left(\frac{\omega}{\beta^2} \sqrt{(x - x_1)^2 - \beta^2 y_1^2}\right) dx_1 dy_1, \quad (2.8) \end{aligned}$$

where  $K$  is the triangle obtained in the intersection of the inverse Mach cone emanating from the point  $(x, y)$  with the whole plate (Fig. 2) and  $\beta = \sqrt{M^2 - 1}$ .

Thus, substituting the expression (2.8) with the pinning boundary conditions into the equation of motion of the plate (2.6), we arrive at an integro-differential problem for finding complex eigenvalues  $\omega$ . Note that the eigenvalue  $\omega$  enters the equation in a complicated way: both algebraically and through the kernel of the integral operator. The system is unstable if and only if at least one of the eigenfrequencies  $\omega_n$  lies in the upper complex half-plane  $\text{Im } \omega_n > 0$ .

The results of numerical solution of the indicated eigenvalue problem will be given below in Section 5. Now we consider another approach to the solution of the same problem.

### 3. ASYMPTOTIC METHOD FOR ONE-DIMENSIONAL SYSTEMS

**3.1. General solution to the initial–boundary value problem.** Consider an arbitrary one-dimensional system with spatial coordinate  $x$  and unknown functions  $u_1(x, t), \dots, u_n(x, t)$ . Suppose that the linearized system of equations for perturbations is a system of partial differential



To determine  $C_m$ , we substitute (3.5) into the boundary conditions (3.3). We obtain a system of linear algebraic equations for  $C_m$  of the following form:

$$\begin{pmatrix} a_{11}e^{-ik_1L/2} & a_{12}e^{-ik_2L/2} & \dots & a_{1N}e^{-ik_NL/2} \\ \dots & \dots & \dots & \dots \\ a_{s1}e^{-ik_1L/2} & a_{s2}e^{-ik_2L/2} & \dots & a_{sN}e^{-ik_NL/2} \\ a_{(s+1)1}e^{ik_1L/2} & a_{(s+1)2}e^{ik_2L/2} & \dots & a_{(s+1)N}e^{ik_NL/2} \\ \dots & \dots & \dots & \dots \\ a_{N1}e^{ik_1L/2} & a_{N2}e^{ik_2L/2} & \dots & a_{NN}e^{ik_NL/2} \end{pmatrix} \begin{pmatrix} C_1 \\ \dots \\ C_s \\ C_{s+1} \\ \dots \\ C_N \end{pmatrix} = \begin{pmatrix} a_1^*(-L/2, \omega) \\ \dots \\ a_s^*(-L/2, \omega) \\ a_{s+1}^*(L/2, \omega) \\ \dots \\ a_N^*(L/2, \omega) \end{pmatrix}.$$

Here  $a_{ij} = a_{ij}(k_j(\omega), \omega)$ , and the right-hand side is defined by the choice of the particular solution  $U_j^*(x, \omega)$ .

Denote the matrix of the system by  $A$  and the matrix in which the  $m$ th column is replaced with the right-hand side by  $A_m$ . Then, by Cramer's rule we have  $C_m = |A_m|/|A|$ , which yields a solution to the boundary value problem:

$$U_j(x, \omega) = U_j^*(x, \omega) + \frac{1}{|A|} \sum_{m=1}^N |A_m| b_{jm}(\omega) e^{ik_m(\omega)x}.$$

Applying the inverse Laplace transform, we obtain a solution satisfying the initial and boundary conditions:

$$u_j(x, t) = \frac{1}{2\pi} \int_{\Gamma} \left[ U_j^*(x, \omega) + \frac{1}{|A|} \sum_{m=1}^N |A_m(\omega)| b_{jm}(\omega) e^{ik_m(\omega)x} \right] e^{-i\omega t} d\omega. \tag{3.6}$$

The integration is performed along a line  $\Gamma$  parallel to the real axis that lies sufficiently high in the complex  $\omega$ -plane:  $-\infty < \text{Re } \omega < \infty, \text{Im } \omega = \text{const} > P$ . The integral (3.6) is calculated by moving the integration contour downward to the domain  $\text{Im } \omega \rightarrow -\infty$ , finding the poles of the integrand, and applying the residue theorem:

$$u_j(x, t) = \sum_{n=1}^{\infty} i \left( \frac{d|A(\omega_n)|}{d\omega} \right)^{-1} \sum_{m=1}^N |A_m(\omega_n)| b_{jm}(\omega_n) e^{i(k_m(\omega_n)x - \omega_n t)}. \tag{3.7}$$

Here the cuts emanating from the branch points of the function  $k(\omega)$  do not contribute to the value of the integral (3.7), because bypassing the cut on different sides leads only to renumbering the branches  $k_m(\omega)$  rather than to changing the values of the integrand. The countable set of eigenfrequencies  $\omega_n$  is determined by the equation

$$|A(\omega)| = 0. \tag{3.8}$$

The solution (3.7) is obtained in the case when the behavior of perturbations of the physical system is described by a system of partial differential equations. In this case, the dispersion equation (3.4) contains no branch points, and the solution has only discrete frequency spectrum. In the case of a plate streamlined by a gas, the system of equations has a form different from (3.1) (because only the plate has a finite size, while the gas flows along the whole  $x$ -axis), and the dispersion equation has branch points. In this case, the solution (3.7) has an additional continuous spectrum, which arises due to taking into account the cut connecting the branch points in the complex  $\omega$ -plane. One can show that the continuous spectrum in this particular case is real and the stability of the solution obtained is determined only by the discrete frequency spectrum.

Note that the calculations performed here are valid not only for systems described by partial differential equations but also for arbitrary linear homogeneous systems whose properties are invariant along the  $x$ -axis. Such systems always have solutions of traveling wave type, from which one can obtain, by superposition, a solution satisfying the boundary conditions.

**3.2. Global and one-sided instability.** Suppose that the width of the system is large enough ( $L \gg 1$ ). It turns out that in this case one can analyze the behavior of the eigenfrequencies  $\omega_n$  in the general form and obtain the criterion found by Kulikovskii [7] (see also [12, § 65]) for the asymptotic stability of the system.

First, we consider the general properties of the solutions of the dispersion equation for the infinite system,

$$\mathcal{D}(k, \omega) = 0.$$

We will assume that the system is evolutionary, i.e., the quantity  $P = \max_{k \in \mathbb{R}} \text{Im } \omega_j(k)$  exists and is finite. Then, for  $\text{Im } \omega > P$ , all the solutions  $k_j = k_j(\omega)$  are complex. Let us number them in the order of decreasing imaginary part for large  $\text{Im } \omega$  and split them into two groups:  $\text{Im } k_j > 0$ ,  $j = 1, \dots, s$ , and  $\text{Im } k_j < 0$ ,  $j = s + 1, \dots, N$ . We will call the waves corresponding to wavenumbers from the first (second) group waves moving *from left to right* (respectively, *from right to left*).

Consider the frequency equation (3.8):

$$\begin{vmatrix} a_{11}e^{-ik_1L/2} & a_{12}e^{-ik_2L/2} & \dots & a_{1N}e^{-ik_NL/2} \\ \dots & \dots & \dots & \dots \\ a_{s1}e^{-ik_1L/2} & a_{s2}e^{-ik_2L/2} & \dots & a_{sN}e^{-ik_NL/2} \\ a_{(s+1)1}e^{ik_1L/2} & a_{(s+1)2}e^{ik_2L/2} & \dots & a_{(s+1)N}e^{ik_NL/2} \\ \dots & \dots & \dots & \dots \\ a_{N1}e^{ik_1L/2} & a_{N2}e^{ik_2L/2} & \dots & a_{NN}e^{ik_NL/2} \end{vmatrix} = 0, \tag{3.9}$$

where  $a_{ij} = a_{ij}(k_j(\omega), \omega)$ . For  $L \rightarrow \infty$ , the leading term of this determinant is the product of the exponential factor

$$e^{-i(k_1(\omega) + \dots + k_s(\omega) - k_{s+1}(\omega) - \dots - k_N(\omega))L/2}$$

and two minors of the matrix  $A$ : one of them has order  $s$  and occupies the upper left corner, and the other has order  $n - s$  and occupies the lower right corner of this matrix. The second leading exponential term differs from the first one by

$$e^{i(k_s(\omega) - k_{s+1}(\omega))L},$$

and its coefficient is the product of the similar minors of the matrix obtained from  $A$  by interchanging the  $s$ th and  $(s + 1)$ th columns. Thus, retaining the leading two terms in equation (3.9), we obtain

$$|A_s| \cdot |A_{N-s}| + |A'_s| \cdot |A'_{N-s}| e^{i(k_s(\omega) - k_{s+1}(\omega))L} = 0. \tag{3.10}$$

The solutions of equation (3.10) for  $L \gg 1$  fall into one of the following two groups.

1. If  $\text{Im } k_s(\omega) \neq \text{Im } k_{s+1}(\omega)$ , then, as  $L \rightarrow \infty$ , equality (3.10) yields

$$|A_s(\omega)| \cdot |A_{N-s}(\omega)| = 0. \tag{3.11}$$

The eigenfrequencies defined by this equation are said to be *one-sided* (the meaning of this term will be explained below). If at least one of these eigenfrequencies has a positive imaginary part, then the system is unstable; in this case, the instability is also said to be *one-sided*.

2. If equation (3.11) is not satisfied, then, as  $L \rightarrow \infty$ , (3.10) necessarily implies the equality

$$\text{Im } k_s(\omega) = \text{Im } k_{s+1}(\omega). \tag{3.12}$$

Equation (3.12) defines a curve  $\Omega$  in the complex  $\omega$ -plane that possesses the following property: in the neighborhood of any of its points, there always exists a frequency that satisfies (3.10), and,

conversely, any such (non-one-sided) frequency lies in the neighborhood of this curve. Thus, the non-one-sided eigenfrequencies, albeit forming a discrete set, are situated near the curve  $\Omega$ ; the greater the length  $L$  of the system, the closer these eigenfrequencies to this curve and the higher their density along the curve. If a part of  $\Omega$  is in the upper half-plane of  $\omega$ , then the eigenfrequencies situated near this part of the curve correspond to unstable perturbations. The spectrum defined by equality (3.12) and the instability due to this spectrum are said to be *global* (the meaning of this term will be explained below).

When deriving equality (3.12), we assumed that the mutual arrangement of  $\text{Im } k_j$  inside each group is not changed under the variation of  $\omega$ . In the general case, the curve  $\Omega$  near which the eigenfrequencies are situated is defined by the equation

$$\min_{1 \leq j \leq s} \text{Im } k_j(\omega) = \max_{s+1 \leq j \leq N} \text{Im } k_j(\omega). \quad (3.13)$$

Thus, for sufficiently large  $L$ , the frequency spectrum is split into one-sided and global ones. The greater  $L$ , namely, the more accurate the transition from (3.9) to (3.10) and then to (3.11) and (3.12), the higher the accuracy of such splitting.

**3.3. Physical meaning of one-sided instability.** Let, for definiteness, the determinant  $|A_s|$  in (3.11) vanish. Consider the semi-infinite system on the interval  $x > -L/2$  subject to the damping condition for  $x \rightarrow +\infty$ . Solving the system of equations for perturbations in the same way as in Subsection 3.1, we obtain a solution in the form (3.5). The difference is that, in view of the damping condition for  $x \rightarrow +\infty$ , in (3.5) one should keep only the  $s$  traveling waves that move away from the boundary  $x = -L/2$  and correspond to the wavenumbers  $k_1, \dots, k_s$ . Substituting the solution (3.5) thus modified into the boundary conditions at  $x = -L/2$ , we obtain a system of linear algebraic equations with the matrix  $A_s$  for determining the amplitudes  $C_j$ . Solving this system and calculating an analog of integral (3.6), we find that the spectrum of eigenfrequencies of the semi-infinite system is determined by the frequency equation

$$|A_s| = 0.$$

When the determinant  $|A_{N-s}|$  vanishes in (3.11), one should consider the semi-infinite system on the interval  $x < L/2$  subject to the damping condition for  $x \rightarrow -\infty$ .

Hence, the one-sided spectrum of a finite system is the union of the spectra of systems that are infinitely long in one of the directions, which explains its name.

Note that the one-sided instability is determined only by the boundary conditions specified separately at the right and left ends of the system and does not depend on the combination of these conditions.

**3.4. Physical meaning of global instability.** Assume for definiteness that the arrangement of  $\text{Im } k_j$  inside each group is not changed under the variation of  $\omega$  and the equation for the curve  $\Omega$  is given by (3.12).

Suppose that at one end of the system, say, at  $x = -L/2$ , a perturbation is excited in the form of  $s$  traveling waves moving away from this end:

$$\sum_{j=1}^s C_s e^{i(k_j x - \omega t)}.$$

When these waves reach the right end  $x = L/2$ , the amplitude of one of them, namely, that of the  $s$ th wave, is much greater than the amplitudes of the other waves, because  $k_j$  are numbered in the order of decreasing imaginary parts. Hence, one can neglect the other waves when determining the amplitudes of the waves reflected from the right end. When the  $N - s$  reflected waves traveling

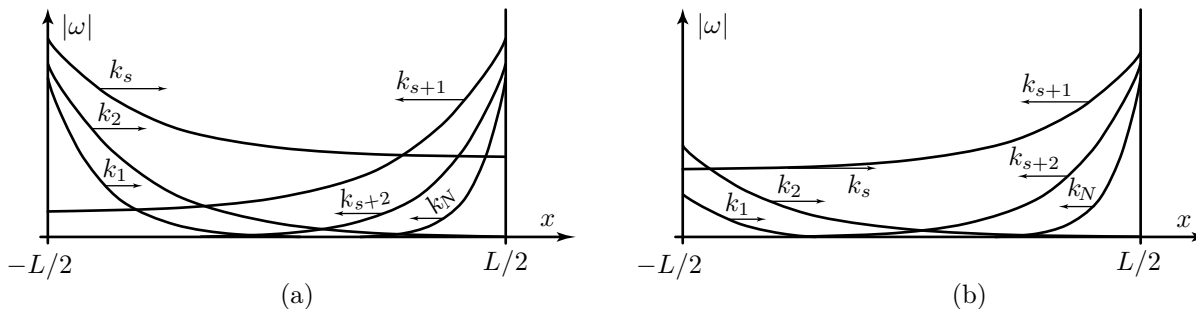


**Fig. 3.** (a) Hierarchy of waves in a system of finite length, and (b) mutual transformation of  $k_s$  and  $k_{s+1}$  into each other under reflections from boundaries in an eigenfunction. The arrows indicate the propagation directions of waves.

away from the right end return to the left end, for a similar reason one can neglect the amplitudes of all waves except the  $(s + 1)$ th one.

Thus, for large  $L$ , two waves traveling in opposite directions, namely, the  $s$ th and  $(s + 1)$ th ones, play a dominant role in the reflection process. This situation is illustrated in Fig. 3a.

Let us calculate the amplitudes of these waves at different instants of time. When the wave  $C_s e^{i(k_s x - \omega t)}$  excited at the left end reaches the right end, its amplitude is  $C_s e^{-\text{Im } k_s L/2}$  (the coefficient  $e^{-i\omega t}$  can be ignored because it is the same for all waves). Upon reflection, this wave turns into the wave  $A_{s,s+1} C_s e^{-\text{Im } k_s L/2} e^{\text{Im } k_{s+1} L/2} e^{i(k_{s+1} x - \omega t)}$ , where  $A_{s,s+1}$  is the reflection coefficient of the  $s$ th wave into the  $(s + 1)$ th one at the right end. When the latter wave reaches the left end, its amplitude becomes  $A_{s,s+1} C_s e^{-\text{Im } k_s L/2} e^{\text{Im } k_{s+1} L}$ . Upon reflection, it turns into the wave  $A_{s+1,s} A_{s,s+1} C_s e^{-\text{Im } k_s L/2} e^{\text{Im } k_{s+1} L} e^{-\text{Im } k_s L/2} e^{i(k_s x - \omega t)}$ , where  $A_{s+1,s}$  is the reflection coefficient of the  $(s + 1)$ th wave into the  $s$ th one at  $x = -L/2$ .

If the amplitude and phase of the  $s$ th wave after two reflections coincide with the original ones, the process described will be cyclically repeated, i.e., it will represent an eigenfunction. The condition of invariance of the amplitude has the form

$$A_{s+1,s} A_{s,s+1} e^{\text{Im}(k_{s+1} - k_s)L} = 1.$$

For large  $L$ , this condition can be satisfied only if  $\text{Im } k_s(\omega) \approx \text{Im } k_{s+1}(\omega)$ , i.e., for  $\omega$  lying in the neighborhood of the curve (3.12). On the other hand, in the neighborhood of any point defined by equality (3.12), one can find a frequency at which not only the amplitude but also the phase of the wave after double reflection coincides with the original amplitude and phase, i.e., the process of reflections represents a natural oscillation.

Thus, the global eigenfunctions are composed of the two most amplified (most slowly damped) waves that travel in opposite directions and turn into each other at the ends of the system (Fig. 3b). One can see from (3.12) that the spectrum of global eigenfrequencies does not depend on specific boundary conditions at  $x = \pm L/2$  but is determined only by the character of the system in the interval  $-L/2 < x < L/2$ . This is why we use the term ‘‘global.’’

**3.5. Weak global instability.** In the case of weak instability, we can present a simpler mechanism of formation of an eigenfunction.

Suppose that one of the parameters of the problem, which we denote by  $\mu \in \mathbb{R}$ , is small and, moreover, the system is neutrally stable for  $\mu = 0$ . The dispersion equation has the form

$$\mathcal{D}(k, \omega, \mu) = 0,$$

and its solutions are  $k_j = k_j(\omega, \mu)$ . Consider a real eigenfrequency  $\omega_R \in \mathbb{R}$  lying on the curve  $\Omega$  for  $\mu = 0$ , i.e., such that

$$\text{Im } k_s(\omega_R, 0) = \text{Im } k_{s+1}(\omega_R, 0). \tag{3.14}$$

Let us supplement this frequency with an increment  $i\omega_I$ , where  $\omega_I \in \mathbb{R}$ ,  $|\omega_I| \ll 1$ , and find an  $\omega_I$  such that this frequency lies on the curve  $\Omega$  for  $\mu \neq 0$ ,  $|\mu| \ll 1$ . We have

$$k_j(\omega_R + i\omega_I, \mu) = k_j(\omega_R, 0) + i \frac{\omega_I}{g(\omega_R)} + \Delta(k_j(\omega_R, 0), \omega)\mu,$$

$$\Delta = \left. \frac{\partial k_j}{\partial \mu} \right|_{\mu=0} = - \left. \frac{\partial \mathcal{D}}{\partial \mu} \left( \frac{\partial \mathcal{D}}{\partial k_j} \right)^{-1} \right|_{\mu=0}, \quad g(\omega_R) = \left. \left( \frac{\partial k_j}{\partial \omega} \right)^{-1} \right|_{\mu=0}.$$

The equation  $\text{Im } k_s(\omega_R + i\omega_I, \mu) = \text{Im } k_{s+1}(\omega_R + i\omega_I, \mu)$  for the curve  $\Omega$  reduces to the following expression for the frequency increment:

$$\omega_I(\omega_R) = \mu \left( \text{Re } \frac{\partial k_s}{\partial \omega} - \text{Re } \frac{\partial k_{s+1}}{\partial \omega} \right)^{-1} \text{Im}(\Delta(k_{s+1}, \omega_R) - \Delta(k_s, \omega_R))\mu.$$

By definition,  $\text{Im } k_s$  should increase and  $\text{Im } k_{s+1}$  decrease with increasing  $\omega_I$ ; hence,

$$\text{Re } \frac{\partial k_s}{\partial \omega} > 0, \quad \text{Re } \frac{\partial k_{s+1}}{\partial \omega} < 0.$$

The system is unstable when  $\omega_I(\omega_R) > 0$  for at least one real  $\omega_R$ , which implies the instability criterion

$$\text{Im } \Delta(k_{s+1}, \omega_R) > \text{Im } \Delta(k_s, \omega_R). \tag{3.15}$$

The physical meaning of this criterion is as follows. When  $\mu = 0$ , the amplifications of the wave  $e^{ik_s x}$  traveling from left to right and of the wave  $e^{ik_{s+1} x}$  traveling from right to left coincide, which is expressed by equality (3.14). For  $\mu \neq 0$  and the same real frequency  $\omega_R$ , these amplifications become different, because  $\text{Im } \Delta(k_s, \omega_R) \neq \text{Im } \Delta(k_{s+1}, \omega_R)$  in the general case. If the amplification of the wave traveling in one direction exceeds the damping of the wave traveling in the opposite direction (which is expressed by condition (3.15)), then, as a result of propagation and mutual reflection of these two waves, for *real* frequency, the amplitude will increase in each cycle of reflections. As a result, the perturbation will exponentially increase, which means the instability.

This amplifying process of reflections does not represent an eigenfunction, because condition (3.12) is not satisfied for real  $\omega_R$  and  $\mu \neq 0$ . However, an eigenfunction can be obtained by adding an increment  $i\omega_I(\omega_R)$  to the frequency. In this case, the process of reflections is not amplified; however, amplification will occur due to the presence of a positive imaginary part of the frequency. Thus, in the case of weak global instability, two equivalent representations of the formation of an eigenfunction are possible: amplifying reflections for real frequency and reflections at a frequency shifted by  $i\omega_I$  under which the wave amplitude is preserved.

#### 4. GLOBAL INSTABILITY OF AN ELASTIC PLATE IN A GAS FLOW

**4.1. Results of the analysis of the curve  $\Omega$ .** So far we have considered the instability criterion for systems of large length in the general form. Consider the results of its application to the stability problem of a plate in the form of a strip (see Fig. 1a) in a gas flow [21, 22]. For waves in an infinite plate, the dispersion equation obtained from the solution of system (2.6), (2.7) has the form

$$(Dk^4 + M_w^2 k^2 - \omega^2) - \mu \frac{(\omega - Mk)^2}{\sqrt{k^2 - (\omega - Mk)^2}} = 0. \tag{4.1}$$

The first term expresses the contribution of elastic and inertia forces of the plate, and the second expresses the effect of the gas flow. The radiation condition requires the choice of the following branch of the square root:

$$\text{Re} \sqrt{k^2 - (\omega - Mk)^2} > 0, \quad \text{Im } \omega \rightarrow +\infty.$$

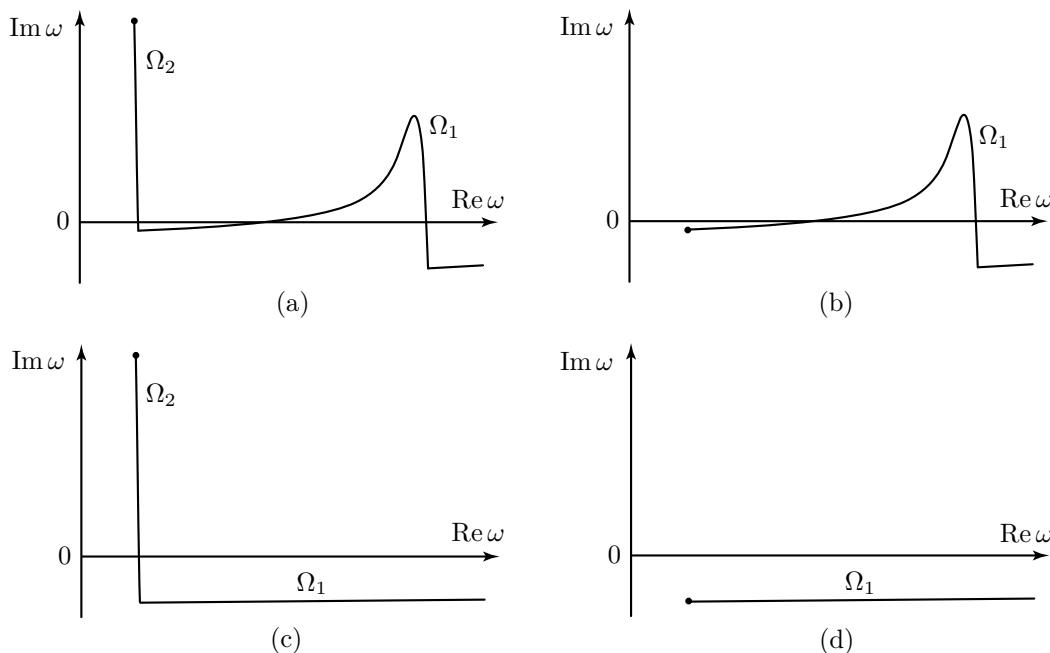


**Fig. 4.** Typical shape of the curve  $\Omega$ : (a) in the case of simultaneous single-mode and coupled flutter, (b) in the case of single-mode flutter alone, (c) in the case of coupled flutter alone, and (d) in the case of stability. The circle indicates the end of the curve  $\Omega$ , which is the branch point of  $k_2$  and  $k_4$  (a, c) or of  $k_2$  and  $k_3$  (b, d).

The dispersion equation (4.1) has four roots:  $k_1$  and  $k_2$ , which belong to the first group, and  $k_3$  and  $k_4$ , which belong to the second. For  $\mu = 0$ , these roots correspond to flexural waves that propagate along the plate in vacuum. The analysis shows that, first, there are no one-sided eigenfunctions under typical clamping, pinning, and free-edge boundary conditions. Second, global instability can take place [21, 22], and the curve  $\Omega$  consists in the general case of two parts,  $\Omega_1$  and  $\Omega_2$ , which correspond to the two different mechanisms of instability (Fig. 4). The results in [21, 22] were obtained under the assumption that the parameter  $\mu$  is small, which almost always holds for realistic parameters of the problem: the gas density is 1000 and more times less than the densities of typical engineering materials, so that  $\mu \lesssim 10^{-3}$ .

In the range of sufficiently high frequencies  $\omega \gtrsim \mu^{2/3}$ , there is a curve  $\Omega_1$  defined by the relation

$$\text{Im } k_1 > \text{Im } k_2(\omega) = \text{Im } k_3(\omega) > \text{Im } k_4,$$

where  $k_2$  and  $k_3$  correspond in the absence of gas to sinusoidal waves traveling in opposite directions. For

$$M > M_w + 1, \tag{4.2}$$

this curve has a region lying in the upper half-plane of  $\omega$ , which has a characteristic “hump” corresponding to the most rapidly growing eigenfunctions (Fig. 5). Namely, under condition (4.2), the curve enters the upper half-plane in the interval  $\omega^{**} < \text{Re } \omega < \omega^*$ , where

$$\omega^* = (M - 1) \sqrt{\frac{(M - 1)^2 - M_w^2}{D}},$$

$$\omega^{**} = \sqrt{\frac{(M^2 + 1 - \sqrt{4M^2 + 1})(M^2 + 1 - \sqrt{4M^2 + 1} - M_w^2)}{D}},$$

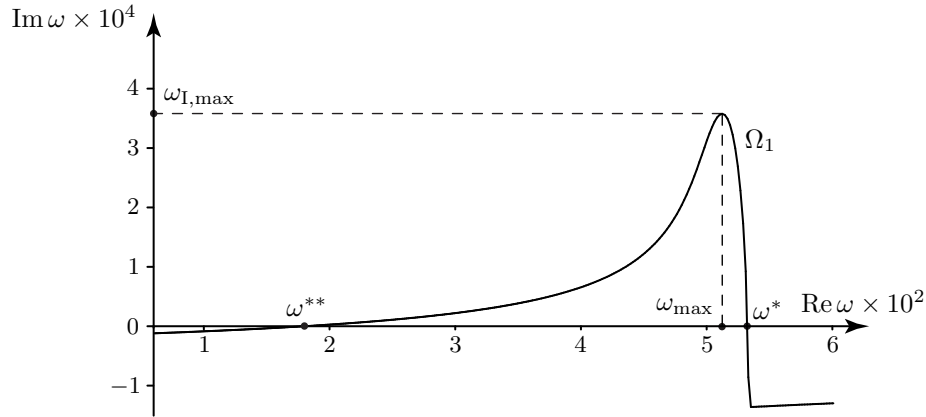


**Fig. 5.** Curve  $\Omega_1$  for the parameters (4.3).

which corresponds to the phase velocity range

$$\sqrt{M^2 + 1 - \sqrt{4M^2 + 1}} < c < M - 1.$$

Here  $\omega^{**}$  is real only for  $M > \sqrt{\sqrt{4M_w^2 + 1} + M_w^2 + 1}$ ; if

$$1 < M < \sqrt{\sqrt{4M_w^2 + 1} + M_w^2 + 1},$$

then the curve  $\Omega_1$  lies in the upper half-plane on the whole interval  $0 < \text{Re } \omega < \omega^*$ . The frequency  $\omega_{\max}$  at which  $\text{Im } \omega$  attains its maximum lies close to  $\omega^*$ :  $|\omega_{\max} - \omega^*| \sim \mu^{2/3}$ ; therefore, with a high degree of accuracy, we can assume that  $\omega_{\max} \approx \omega^*$ . The maximum growth rate of perturbations (“height of the hump”) is

$$\begin{aligned} \omega_{I,\max}(M, M_w, D, \mu) &= \mu^{2/3} \frac{\sqrt{3}}{8} \left( \frac{(M-1)^2 - M_w^2}{D} \right)^{1/6} \frac{(2(M-1)^2 - M_w^2)^{1/3}}{(M-1)^{4/3}} \\ &\quad - \mu \frac{(2M-1)^2}{4(M-1)\sqrt{(2M-1)^2 - 1}}. \end{aligned}$$

Outside the range  $\omega^{**} < \text{Re } \omega < \omega^*$ , the curve  $\Omega_1$  lies in the domain  $\text{Im } \omega < 0$ ; as  $|\omega| \rightarrow \infty$ , it asymptotically approaches the horizontal axis from below. In the absence of gas flow, the curve  $\Omega_1$  coincides with the horizontal axis and describes all possible natural oscillations of the plate in vacuum; therefore, the eigenfunctions with frequencies close to  $\Omega_1$  represent the eigenmodes in vacuum modified by a gas flow.

An example of calculated curve  $\Omega_1$  is demonstrated in Fig. 5 for the parameters  $M = 1.5$ ,  $M_w = 0$ , and

$$D = 23.9, \quad \mu = 1.2 \times 10^{-4}, \tag{4.3}$$

where the values of  $D$  and  $\mu$  correspond to a steel plate in an air flow at an altitude of 3000 m or to an aluminum plate at an altitude of 11 000 m above the sea level.

Following the curve  $\Omega$  to the left, one may face two situations. If the tension  $M_w$  is high enough, then the curve ends with a branch point of the roots  $k_2 = k_3$ ; it does not contain parts other than  $\Omega_1$  (see Figs. 4b and 4d). In the case of tension

$$M_w < M_w^{\text{cr}} = \left( \frac{\sqrt{54}}{4} \right)^{1/3} \left( \frac{\mu M^2}{\sqrt{M^2 - 1}} \right)^{1/3} D^{1/6}, \tag{4.4}$$

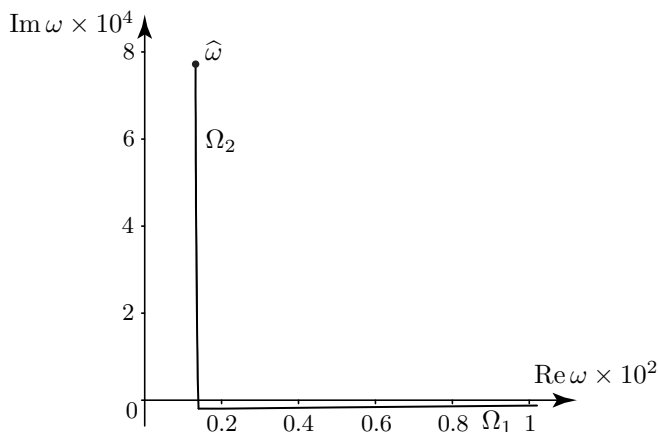


Fig. 6. Curve  $\Omega_2$  for the parameters (4.3).

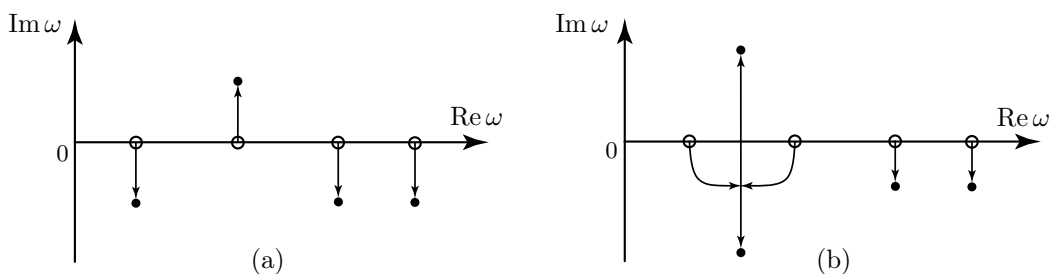


Fig. 7. Transition to instability: (a) for single-mode flutter and (b) for coupled flutter.

a corner point of the curve  $\Omega$  arises at which  $\text{Im } k_2 = \text{Im } k_3 = \text{Im } k_4$ . The further continuation of  $\Omega$  is given by the relation

$$\text{Im } k_1 > \text{Im } k_2 = \text{Im } k_4 > \text{Im } k_3,$$

which determines the part  $\Omega_2$  (Fig. 6). It is situated almost vertically and ends with the branch point of  $k_2 = k_4$  (Figs. 4a and 4c). In the absence of tension, i.e., for  $M_w = 0$ , the location of this branch point is found explicitly:

$$\hat{k} = \left( \frac{\mu M^2}{\sqrt{M^2 - 1}} \right)^{1/3} (4D)^{-1/3} e^{-i\pi/6}, \quad \hat{\omega} = \frac{\sqrt{3}}{2} \left( \frac{\mu M^2}{\sqrt{M^2 - 1}} \right)^{2/3} (4D)^{-1/6} e^{i\pi/6}.$$

For  $M_w = M_w^{cr}$ , there is an intermediate state: the curve  $\Omega_2$  consists of one triple branch point  $k_2 = k_3 = k_4$ , which is also an endpoint of the curve  $\Omega_1$ , and the branch point itself in the  $\omega$ -plane is real in this case and is given by

$$\hat{k} = -\frac{i}{2} \left( \frac{\mu M^2}{\sqrt{M^2 - 1}} \right)^{1/3} D^{-1/3}, \quad \hat{\omega} = \frac{\sqrt{3}}{4} \left( \frac{\mu M^2}{\sqrt{M^2 - 1}} \right)^{2/3} D^{-1/6}.$$

When condition (4.4) is satisfied but (4.2) is not, the curve  $\Omega_1$  lies completely in the lower half-plane and  $\Omega$  looks as shown in Fig. 4c.

**4.2. Behavior of the eigenmodes of a plate in a gas flow.** Thus, there can exist two instability regions defined by the criteria (4.2) and (4.4), respectively. A more detailed analysis has shown that they correspond to two different physical mechanisms of instability, called single-mode flutter and coupled flutter (Fig. 7). In single-mode flutter, under the action of the flow, the eigenfrequencies of the plate are shifted from the real axis (where they are in the absence of the flow) to the upper half-plane; i.e., a weak (on the order of  $\mu$ ) aerodynamic amplification of

oscillations arises, which is also called negative aerodynamic damping (Fig. 7a). In the coupled type of flutter, two eigenfrequencies approach each other, nearly merge together, and then move away in opposite almost vertical directions: one moves downward, which corresponds to a strongly damped mode, and the other moves upward, which corresponds to a growing mode (Fig. 7b). Thus, the criteria (4.2) and (4.4) give the asymptotic boundaries of each type of flutter as  $L \rightarrow \infty$ . An important fact is that there are no other types of flutter, because the curve  $\Omega$  can have only these two regions in the upper half-plane.

The asymptotic criterion of single-mode flutter (4.2) can be rewritten as an instability criterion for each eigenmode separately. In the case of a weak effect of the flow on the plate, the eigenfrequencies of the plate in the flow are in the neighborhood of the frequencies of the plate in vacuum. On the other hand, they are situated near the curve  $\Omega_1$ , which deviates little from the real axis (by a value on the order of  $\mu$ ). Thus, we can approximately assume that  $\text{Re } \omega_n$  coincide with the frequencies of the plate in vacuum  $\omega_{0n}$  and find  $\text{Im } \omega_n$  from the equation of the curve  $\Omega_1$ . The variation of the length  $L$  of the plate leads to the variation in  $\text{Re } \omega_n$ , and the frequencies will move in the complex plane along  $\Omega_1$  as beads threaded on a rigid wire in the form of this curve. In particular, for a plate simply supported on both sides we have

$$\text{Re } \omega_n \approx \omega_{0n} = \frac{\pi n}{L} \sqrt{D \left( \frac{\pi n}{L} \right)^2 + M_w^2}.$$

If the plate is short enough, then all  $\text{Re } \omega_n > \omega^*$  and the plate is stable. As the length  $L$  of the plate increases, the eigenfrequencies move to the left. For certain lengths  $L$ , the first frequency passes through the “hump” of the curve  $\Omega_1$ , which corresponds to flutter in the first mode; then the second frequency passes through the “hump,” and so on. The instability in the  $n$ th mode corresponds to the situation when the frequency  $\omega_n$  lies between  $\omega^{**}$  and  $\omega^*$ ; this yields the following range of Mach numbers corresponding to instability in this mode:

$$M_n^* < M < M_n^{**}, \tag{4.5}$$

$$M_n^* = 1 + \sqrt{\lambda_n}, \quad M_n^{**} = \sqrt{1 + \lambda_n + \sqrt{4\lambda_n + 1}}, \quad \lambda_n = \frac{\sqrt{4D\omega_{0n}^2 + M_w^4} + M_w^2}{2}. \tag{4.6}$$

In the domain of single-mode flutter, different modes do not interact with each other and have the same structure as the modes in vacuum.

In contrast to the case of single-mode flutter, the stability boundary of coupled flutter cannot be obtained by the asymptotic method in any form analogous to (4.5), because the effect of the flow on the eigenfrequencies becomes essential and the assumption that  $\text{Re } \omega_n \approx \omega_{0n}$  is not valid any longer. The violation of the criterion (4.4) only yields conditions under which coupled flutter does not arise for arbitrarily large length of the plate; however, if this criterion is satisfied, then without a more detailed analysis it is impossible to determine the length  $L$  for which the transition to coupled flutter occurs.

### 5. NUMERICAL ANALYSIS AND COMPARISON WITH ASYMPTOTIC RESULTS

In the one-dimensional problems the accuracy estimate of the asymptotic method is related to the damping rate of those waves away from the boundaries that do not take part in the formation of eigenfunctions. However, in the present case this approach is insufficient, because the problem in question is not completely one-dimensional: the plate has a finite length, whereas the domain of gas flow is infinite. Therefore, it is most expedient to compare the asymptotic results with a numerical solution of the eigenvalue problem (2.6), (2.8). Such a comparison was carried out in [25, 27] for the two-dimensional problem (see Fig. 1a) solved by the Bubnov–Galerkin method, with a detailed description of the numerical method and analysis of convergence.

**5.1. Comparison of results for an untensioned plate.** First, consider the results for a plate without tension, i.e.,  $M_w = 0$ , for the dimensionless parameters (4.3). In Fig. 8, the solid lines demonstrate the results of calculation of the stability boundaries for the first six oscillation modes in the plane  $(L, M)$ , and the dashed lines show the asymptotic boundaries (4.6). One can see that for sufficiently large  $L$  the results of calculations almost coincide; moreover, just as in (4.6),  $M_n^* \rightarrow 1$  and  $M_n^{**} \rightarrow \sqrt{2}$  as  $L \rightarrow \infty$ . For small and moderate  $L$ , there are two differences. First, the real domains of flutter are bounded as  $L$  decreases: for  $L < 57$  the plate is stable, whereas the asymptotic boundaries are unbounded, with  $M^*, M^{**} \rightarrow \infty$  as  $L \rightarrow 0$ . Second, for  $300 \leq L \leq 350$  there is a boundary of coupled flutter; when crossing it, the boundaries of single-mode flutter in the first two modes vanish, because these modes become “coupled.” However, this does not affect the single-mode flutter in higher order modes, whose instability boundaries are continued toward greater  $L$ .

To understand the nature of single-mode flutter, we consider the motion of eigenfrequencies in the  $\omega$ -plane. For simplicity, we will consider the first four frequencies, because the behavior of higher frequencies is analogous. For  $L = 250$  and  $M = 1.6$ , all frequencies lie in the lower half-plane (Fig. 9), and the corresponding modes are damped. We will reduce the Mach number  $M$  for constant  $L$ . For  $M = M_n^*$  (the upper branch in Fig. 8), the  $n$ th frequency crosses the real  $\omega$ -axis and enters the upper half-plane, and the  $n$ th mode becomes a growing mode. An important feature of this transition to instability is that different frequencies do not approach and do not affect each other. Flutter in each mode occurs independently; therefore, it is called “single-mode” flutter. When  $M$  decreases further, the quantity  $\text{Im}\omega_n$  attains its maximum and then decreases. For  $M = M_n^*$  (the lower branch in Fig. 8), the frequencies again cross the real axis and enter the lower half-plane, and the corresponding modes become damped. Thus, the  $n$ th mode,  $n = 1, \dots, 4$ , is in the domain of single-mode flutter for  $M_n^* < M < M_n^{**}$ .

Next, consider a transition from stability to single-mode flutter and then to coupled flutter as the plate length increases. First, we take  $M = 1.3$  and increase  $L$  from 60 to 400. In Fig. 10 one first can see single-mode flutter, which arises when the boundaries in Fig. 8 are crossed. Then, at  $L \approx 320$ , the first and the second frequencies merge together, after which  $\text{Im}\omega_1$  grows rapidly: from  $4.5 \times 10^{-5}$  for  $L = 320$  to  $4.77 \times 10^{-4}$  for  $L = 400$ , whereas  $\text{Im}\omega_2$  decreases rapidly: from  $2.8 \times 10^{-5}$  for  $L = 320$  to  $-4.08 \times 10^{-4}$  for  $L = 400$ . Since, according to Fig. 8, the transition to coupled flutter for  $M = 1.3$  occurs from the domain of single-mode flutter, the merging occurs in the upper half-plane of the  $\omega$ -plane. Higher frequencies ( $n > 2$ ) remain in the upper half-plane

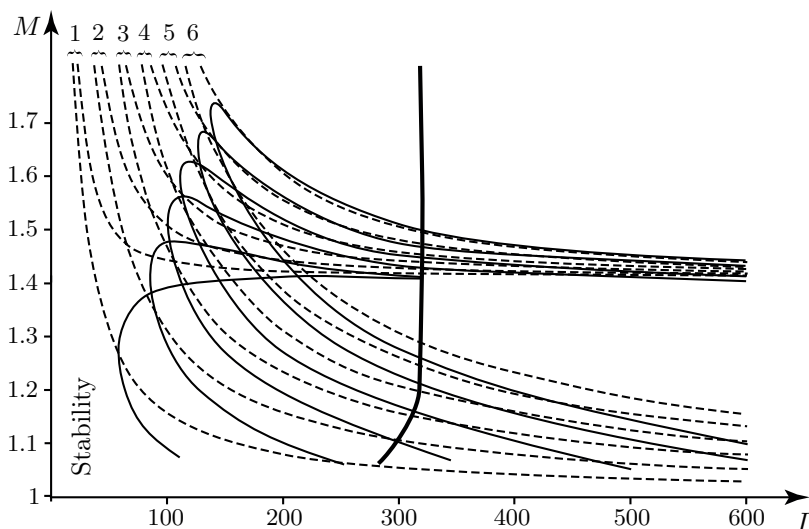


**Fig. 8.** Calculated boundaries of the single-mode flutter in the first six modes (thin solid lines), the asymptotic boundaries (4.6) (dashed lines), and the boundary of the coupled flutter (heavy line).

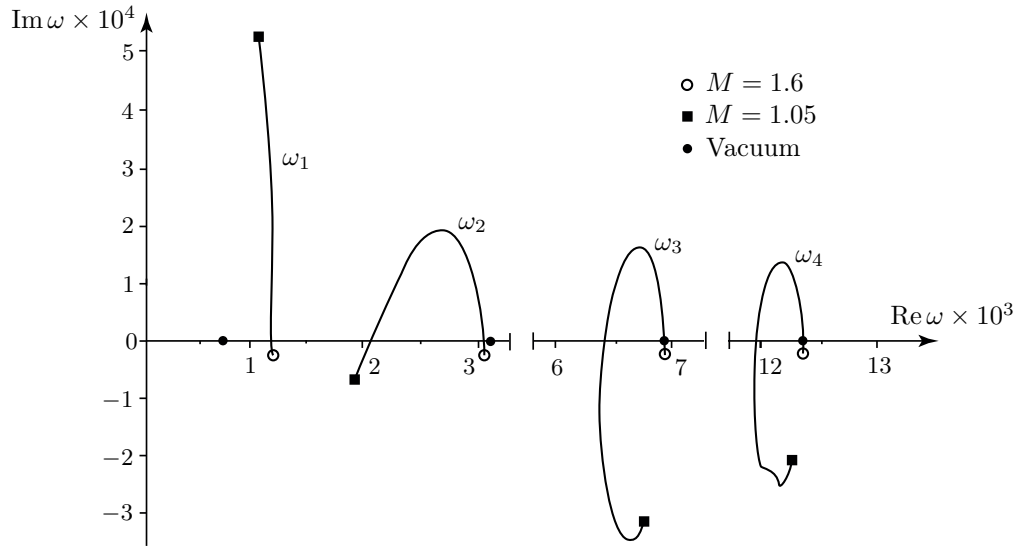


**Fig. 9.** Motion of eigenfrequencies in the complex plane for the parameters (4.3),  $L = 250$ , and  $1.05 \leq M \leq 1.6$ .

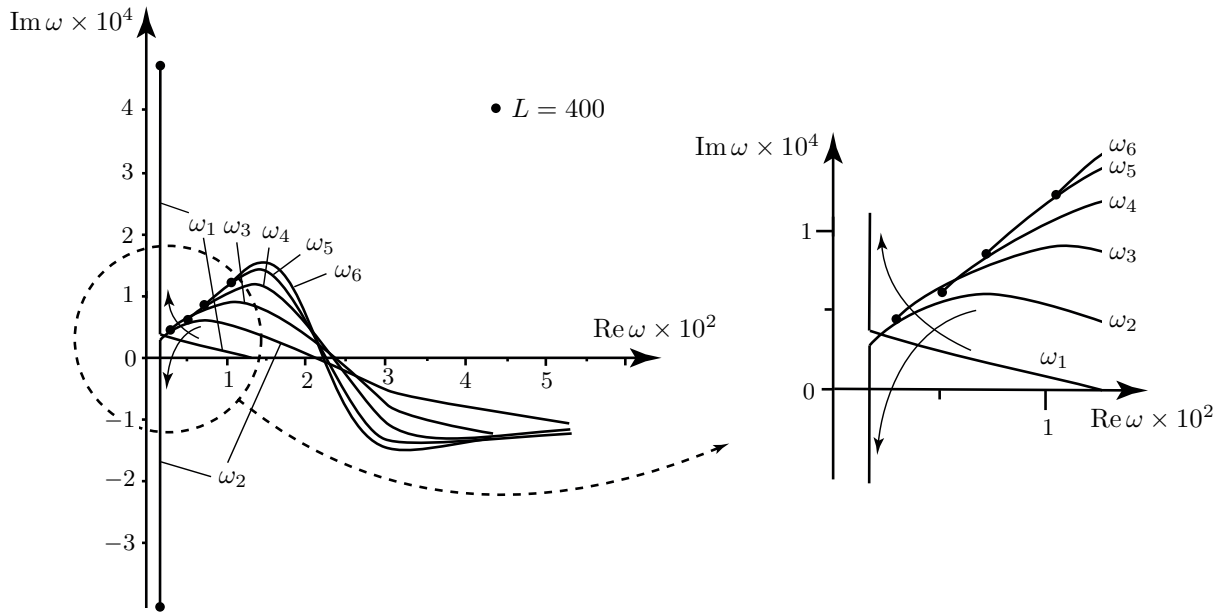


**Fig. 10.** Motion of eigenfrequencies in the complex plane for the parameters (4.3),  $M = 1.3$ , and  $60 \leq L \leq 400$ .

without approaching each other; thus, one simultaneously has coupled flutter in the first two modes and single-mode flutter in higher order modes.

Finally, consider the motion of frequencies when the transition to coupled flutter occurs from the stability region. Take  $M = 1.6$  and increase  $L$  again from 60 to 400 (Fig. 11). For  $110 \leq L \leq 220$ , there is single-mode flutter in modes 4–6 in accordance with the intersection of boundaries in Fig. 8; modes 1–3 are damped for  $L < 321$ . For  $L \approx 321$ , modes 1 and 2 merge together; however, in contrast to the case of  $M = 1.3$ , the merging occurs in the lower half-plane. After merging,  $\text{Im } \omega_1$  increases from  $-2.7 \times 10^{-5}$  for  $L = 321$  to  $4.13 \times 10^{-4}$  for  $L = 400$ , whereas  $\text{Im } \omega_2$  decreases from  $-2.8 \times 10^{-5}$  for  $L = 321$  to  $-4.69 \times 10^{-4}$  for  $L = 400$ . Thus, a transition to coupled flutter occurs. The other frequencies ( $n = 3, \dots, 6$ ) remain in the lower half-plane of  $\omega$ ; i.e., these modes are damped for  $L > 321$ .

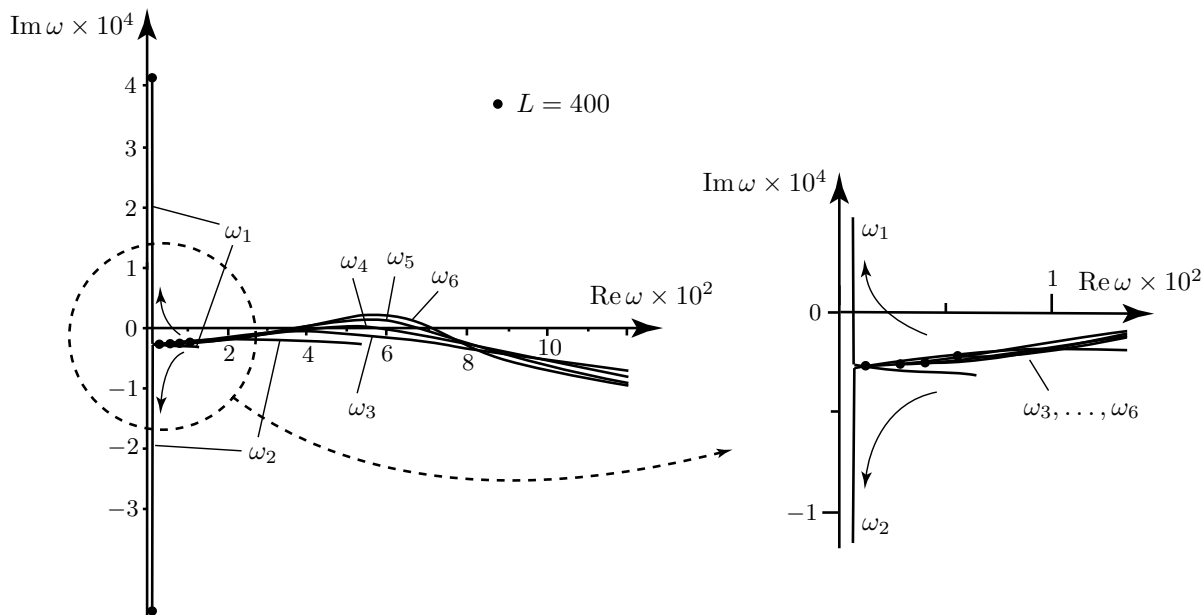


**Fig. 11.** Motion of eigenfrequencies in the complex plane for the parameters (4.3),  $M = 1.6$ , and  $60 \leq L \leq 400$ .

**5.2. The effect of tension on single-mode flutter.** It follows from the asymptotic criterion (4.6) that the Mach numbers for which flutter arises increase significantly as the tension  $M_w$  increases. For example, for a simply supported plate with  $L = 300$ , relations (4.6) show that even for not too high tension of the plate with stress  $\sigma = 129.6 \times 10^6$  Pa, the lower boundary of flutter  $\min_n M_n^*$  increases from 1.051 for an untensioned plate to 1.403. Here and below in calculations we take the parameters (4.3). The table shows the upper and lower boundaries of flutter obtained from (4.6) for the parameters (4.3) as  $L \rightarrow \infty$  (the dependence of  $M_n^*$  and  $M_n^{**}$  on  $n$  disappears as  $L \rightarrow \infty$ ).

The results of calculations for the full problem (2.6), (2.8) are shown in Fig. 12 for  $M_w = 0.2, 0.3, 0.4$ . For  $M_w = 0.2$ , one can see an insignificant variation of the boundaries of flutter, especially in the first mode: the upper branch moves slightly downward, the lower branch, upward, and the left part of the boundary moves to the right. For other modes, the boundaries move slightly upward. The boundary of coupled flutter moves into the domain  $M > 1.8$  and is missing in the figure.

For  $M_w = 0.3$ , the boundary of flutter in the first mode moves into the domain  $L \geq 500$ , and one can only see a small fragment of it in the interval  $500 \leq L < 600$ . For the second mode, the upper branch moves downward, the lower branch, upward, and the left part of the boundary moves to the right. The boundaries for modes 3–6 move to higher values of  $M$ , and the instability region becomes narrower.

For  $M_w = 0.4$ , the boundaries of modes 1 and 2 move into the domain  $L > 600$ , so that they are not seen in Fig. 12. The instability regions in modes 3–6 move toward still greater values of  $M$  and are further narrowed down. The left regions of the boundary for mode 3 are significantly shifted to greater values of  $L$ .

Thus, as  $M_w$  increases, two phenomena are observed in the variation of instability regions. First, in all modes, the instability regions move to higher values of  $M$ , that are close for  $L \rightarrow \infty$  to the values obtained by the asymptotic formulas (4.6) and shown in the table. Second, one can observe a shift of instability regions in lower order modes to greater values of  $L$ ; this phenomenon is not explained by the asymptotic theory.

Variation of the boundaries of single-mode flutter for various tensions of the plate (4.6) with parameters (4.3) as  $L \rightarrow \infty$

$\sigma$ , Pa	$M_w$	$M_n^*$	$M_n^{**}$
0	0.0	1.000	1.414
$8.1 \times 10^6$	0.1	1.100	1.425
$32.4 \times 10^6$	0.2	1.200	1.455
$72.9 \times 10^6$	0.3	1.300	1.502
$129.6 \times 10^6$	0.4	1.400	1.562

**5.3. Comparison of the boundaries of coupled flutter.** Above we considered the boundaries of single-mode flutter for which the transition to instability occurs without interaction between modes. For higher values of  $M$  and  $L$ , the transition to instability occurs through the merging of frequencies, i.e., in the form of coupled flutter (Fig. 8). From the viewpoint of global instability, this occurs when the frequencies are situated near the vertical part of the curve  $\Omega$  (see Fig. 4), i.e., near  $\Omega_2$ . This part exists when condition (4.4) is satisfied.

Inequality (4.4) yields  $M_w$  on the order of  $\mu^{1/3}$ , and, since  $\mu$  is a small quantity, even small tension eliminates coupled flutter. Since the criterion (4.4) does not depend on  $L$ , for  $M_w > M_w^{cr}$  coupled flutter disappears for any plate made of a given material for given thickness and range of Mach numbers, irrespective of how long it is.

Consider the results of calculation of the boundaries of coupled flutter that are shown in Fig. 13 for the parameters (4.3). For every  $L$ , there exists a curve  $M_w = M_w(M)$  such that there is no coupled flutter for  $M_w \geq M_w(M)$  (note that single-mode flutter is possible in this case). The curve

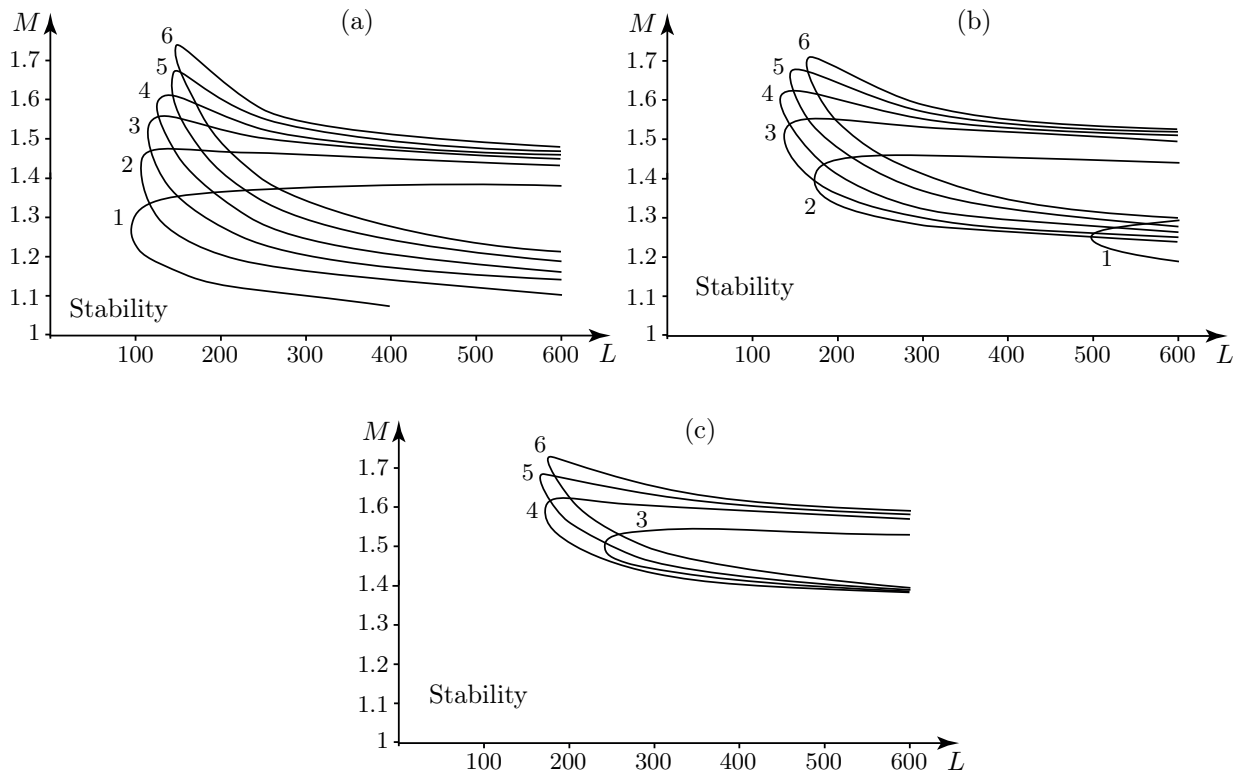


**Fig. 12.** Boundaries of flutter in the first six modes in the plane  $(L, M)$  for the parameters (4.3) and the following values of  $M_w$ : (a) 0.2, (b) 0.3, and (c) 0.4.

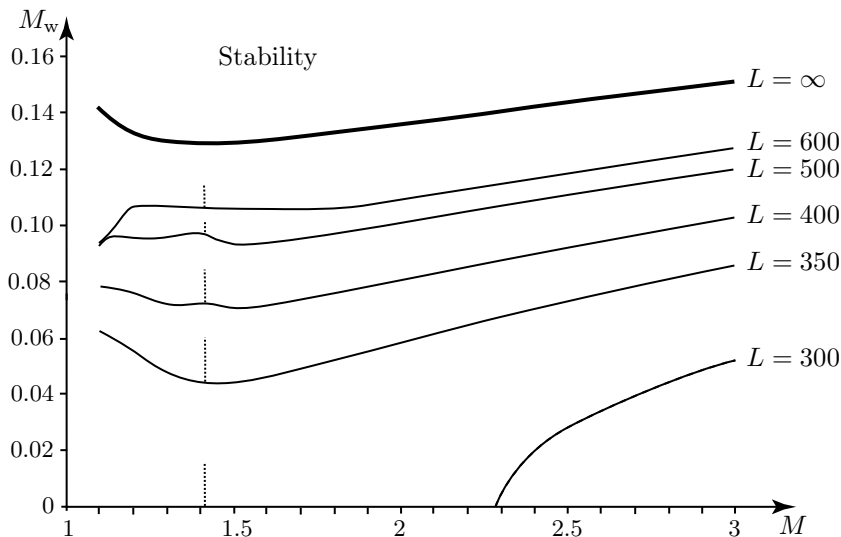


**Fig. 13.** Boundaries of coupled flutter in the plane  $(M, M_w)$  for the parameters (4.3). Thin lines represent the results of calculation for various values of  $L$ , the heavy line shows the asymptotic boundary as  $L \rightarrow \infty$  (4.4), and the dashed lines are the boundaries of single-mode flutter (upper branches).

$M_w = M_w(M)$  obtained by the asymptotic formula (4.4) and denoted as “ $L = \infty$ ” lies above all the curves calculated for finite values of  $L$ , and in this sense it represents the limit boundary of coupled flutter: tension that does not satisfy (4.4) guarantees the absence of coupled flutter for plates of any length. Thus, the asymptotic results correspond to the results obtained from the solution of the full eigenvalue problem.

An interesting feature is that the tension required to suppress coupled flutter is much less than that required to suppress single-mode flutter. Indeed, Fig. 13 shows that  $M_w = 0.15$  is sufficient to eliminate coupled flutter for any length  $L$  of the plate up to  $M = 3.0$ , whereas for the much higher tension  $M_w = 0.4$  there remains a domain of single-mode flutter in Fig. 12 for  $L > 174$  and  $M < 1.74$ .

6. FLUTTER OF RECTANGULAR PLATES: THE ASYMPTOTIC METHOD

The asymptotic method for one-dimensional systems [7; 12, §65] has been generalized to higher dimensions [10]. The idea is as follows: in the case of a domain of sufficiently large size, neglecting the most rapidly damped waves, one can construct closed cycles of reflections of waves that represent eigenfunctions. This generalization was used for constructing the boundaries of single-mode flutter of rectangular plates [23, 26].

**6.1. Effect of gas on natural oscillations.** Consider an eigenmode of a plate in vacuum that is characterized by the numbers  $m$  and  $n$  of half-waves in the directions  $x$  and  $y$ , respectively. For simplicity, we will assume that the plate is simply supported; then an oscillation (standing wave) is defined by the expression

$$w(x, y, t) = \cos(k_x x + \varphi_x) \cos(k_y y + \varphi_y) e^{-i\omega t}. \tag{6.1}$$

In the case of other boundary conditions, the expression (6.1) is valid outside some neighborhood of the edges in view of Bolotin’s dynamic edge effect [2].

Let us represent the oscillation as a superposition of four traveling waves:

$$\begin{aligned} w(x, y, t) &= \frac{1}{4} (e^{i\varphi_x} e^{ik_x x} + e^{-i\varphi_x} e^{-ik_x x}) (e^{i\varphi_y} e^{ik_y y} + e^{-i\varphi_y} e^{-ik_y y}) e^{-i\omega t} \\ &= C_1 e^{i(k_x x + k_y y - \omega t)} + C_2 e^{i(k_x x - k_y y - \omega t)} + C_3 e^{i(-k_x x - k_y y - \omega t)} + C_4 e^{i(-k_x x + k_y y - \omega t)}. \end{aligned} \tag{6.2}$$

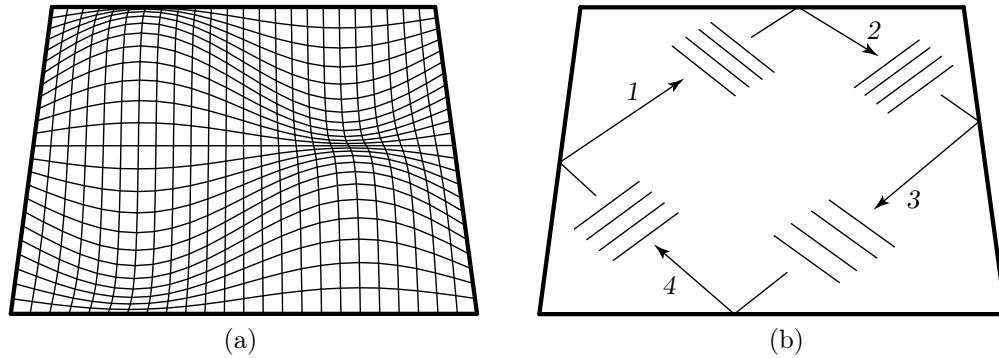


**Fig. 14.** Eigenmode of oscillations of a plate: (a) a standing wave and (b) its representation as a superposition of four traveling waves. The numbers indicate the propagation directions of the waves.

Let us number the propagation directions of waves according to the order of terms in (6.2) (Fig. 14). Then the formation of a standing wave can be represented as follows. At one of the edges, a traveling wave is excited that propagates, say, in direction 1. After successive reflections from the four edges of the plate, it is transformed into waves propagating in directions 2–4. After the last reflection, it turns into the original wave, and then the process is cyclically repeated. After several such cycles, the propagation of the four waves acquires a steady-state character, and their superposition leads to the formation of the standing wave (6.1).

Now, suppose that the plate is exposed to a gas. We will neglect the effect of the plate edges on the perturbation of the gas flow and assume that the flow acts on the traveling waves (6.2) as if they had infinite span. Knowing the effect of gas on such waves, we can easily understand its effect on the natural oscillations as a whole. The effect of the flow on the spatial amplification of infinite-span waves has been analyzed above in the two-dimensional case, i.e., in the case when the direction of the gas flow and the wave vector of the perturbation coincide. Below we present the main results adjusted for the fact that the waves travel at an angle to the gas flow.

Consider the  $j$ th plane wave  $e^{i(k_x x + k_y y - \omega t)}$  with  $\{k_x, k_y\} = \{k \cos(\alpha_j + \theta), k \sin(\alpha_j + \theta)\}$ ,  $j = 1, \dots, 4$ , that travels along an imaginary infinite plate streamlined by a gas. Here  $\alpha_j$  is the angle between the gas velocity vector and the wave vector,  $\theta$  is the angle between the flow direction and the  $x$ -axis, and  $k = \sqrt{k_x^2 + k_y^2}$ ,  $\text{Re } k > 0$ . In the absence of gas,  $k$  is real and positive; in the presence of gas,  $k$  is generally complex. Positive  $\text{Im } k$  correspond to the case when the waves are damped in their propagation direction, while negative  $\text{Im } k$ , to the case when the waves are amplified.

The dispersion equation of the plate–gas system has the form (4.1) with a correction for the fact that the gas velocity vector is projected onto the plane of propagation of the wave:

$$(Dk^4 + M_w^2 k^2 - \omega^2) - \mu \frac{(\omega - Mk \cos \alpha_j)^2}{\sqrt{k^2 - (\omega - Mk \cos \alpha_j)^2}} = 0. \tag{6.3}$$

Denoting by  $k_0(\omega) = k(\omega, 0)$  the length of the wave vector in the absence of gas ( $\mu = 0$ ) and assuming that  $\mu$  is a small parameter, from (6.3) we obtain

$$k(\omega, \mu) = k_0 + \Delta(k_0)\mu,$$

where  $\Delta(k_0)$  is the leading term of the expansion of  $k(\mu)$  for small  $\mu$ .

Now, consider the effect of gas on the natural oscillations. To this end, it is convenient to represent the propagation of a wave as the propagation of its separate regions (Fig. 15). The trajectories of these regions between the edges are segments of straight lines that have one of the four directions (Fig. 14b), with the mirror reflection from the edges. Depending on the oscillation mode, the trajectories may be closed (Figs. 16a and 16b) or open (Fig. 16c). A closed trajectory

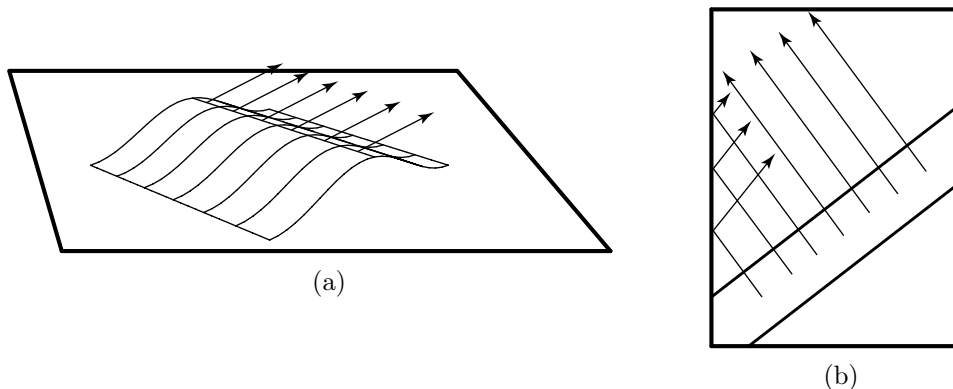


**Fig. 15.** (a) Representation of propagation of a wave as the propagation of its separate regions, and (b) the initial trajectories of these regions.

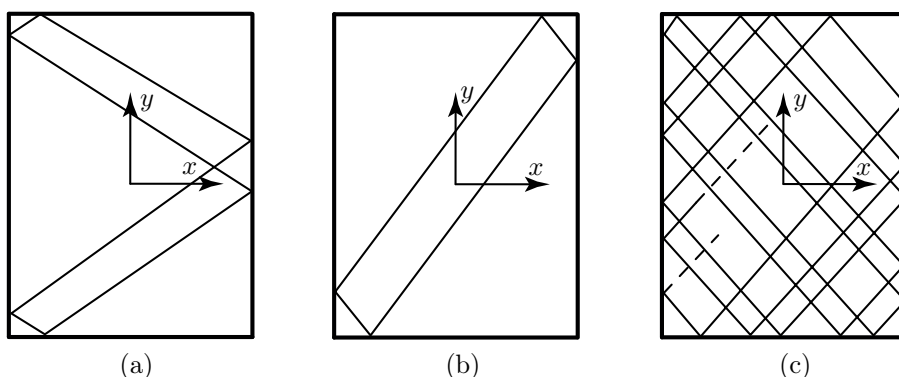


**Fig. 16.** Trajectories of wave regions: (a) a closed trajectory symmetric about one of the coordinate axes, (b) a closed trajectory asymmetric with respect to coordinate axes, and (c) an open trajectory.

is a closed polygonal line. One can easily show that an open trajectory is everywhere dense in the rectangle bounded by the contour of the plate.

By a cycle of reflections of wave regions we will mean a time period during which the trajectories of these regions return to the initial points (in the case of a closed trajectory) or become close to them (in the case of an open trajectory). Calculating the amplitude variation along each trajectory for such a period, we find the amplitude variation for the wave as a whole, because the trajectories cover the whole surface of the plate. If the amplitude amplification is different on different trajectories, then the plane wave ceases to be plane. In this case, diffraction phenomena may arise, which were considered in [26].

Consider some trajectory and calculate the amplitude variation over a cycle of reflections. This variation occurs, first, during the propagation of a wave from one edge to another due to the presence of the imaginary part of the wavenumber (propagation along the segments of the trajectory) and, second, during reflections at the edges of the plate. Taking the initial amplitude equal to 1 and considering successively the amplitude variations during propagation between the edges and under reflections, we obtain the amplitude after a cycle of reflections (it is assumed that  $n$  reflections have occurred during this period of time):

$$\prod_{p=1}^n A_p e^{(-l_1 \operatorname{Im} \Delta(k_1) - l_2 \operatorname{Im} \Delta(k_2) - l_3 \operatorname{Im} \Delta(k_3) - l_4 \operatorname{Im} \Delta(k_4))\mu}. \tag{6.4}$$

Here  $A_i$  are the reflection coefficients at the edges and  $l_j$  are the total distances passed by the trajectory along the  $j$ th direction. Since the amplitude is not changed after the cycle of reflections in

the absence of gas (because the plate is a conservative system in itself), it follows that  $\prod_{p=1}^n A_p = 1$ . Next, it is obvious that  $l_1 = l_3$  and  $l_2 = l_4$  (in the case of an open trajectory, these equalities hold approximately). Therefore, the final condition of amplification of oscillation is as follows:

$$l_1 \operatorname{Im}(\Delta(k_1) + \Delta(k_3)) + l_2 \operatorname{Im}(\Delta(k_2) + \Delta(k_4)) < 0. \tag{6.5}$$

Thus, condition (6.5) allows us to determine the presence or absence of amplitude growth for each trajectory of a given oscillation mode. If such growth occurs on all trajectories, then the oscillation itself is amplified; if the amplitude decreases on all trajectories, then the oscillation is damped. If the amplitude increases on a part of trajectories and decreases on another part, then the resulting behavior is determined by the diffraction of waves; this case is considered in [26].

**6.2. Construction of an eigenfunction.** The above method for calculating the spatial amplification of a wave is completely analogous to the two-dimensional case (Subsection 3.5). Now, let us calculate the rate of temporal growth of the oscillation. To this end, to the frequency  $\omega_R \in \mathbb{R}$  we add a small term  $i\omega_I$  such that the amplitude of the wave region after a cycle of reflections remains unchanged.

Since

$$k(\omega_R + i\omega_I, \mu) = k_0 + \frac{i\omega_I}{g(\omega_R)} + \Delta(k_0)\mu,$$

where  $g(\omega) = (\partial k_0(\omega)/\partial \omega)^{-1}$  is the group velocity of waves, the amplitude variation after a cycle of reflections, calculated by analogy with (6.4), is given by the formula

$$\prod_{p=1}^n A_p e^{(-l_1 \operatorname{Im} \Delta(k_1) - l_2 \operatorname{Im} \Delta(k_2) - l_3 \operatorname{Im} \Delta(k_3) - l_4 \operatorname{Im} \Delta(k_4))\mu - (l_1 + l_2 + l_3 + l_4)\omega_I/g(\omega_R)}.$$

Since this quantity should be equal to 1, the exponent vanishes, which implies that the sought term is given by

$$\omega_I = -\mu g(\omega_R) \frac{l_1 \operatorname{Im}(\Delta(k_1) + \Delta(k_3)) + l_2 \operatorname{Im}(\Delta(k_2) + \Delta(k_4))}{2(l_1 + l_2)}. \tag{6.6}$$

Thus, just as in the two-dimensional case (Subsection 3.5), we have found that the formation of a growing eigenfunction of a rectangular plate can be represented in two ways: either as a growing process of reflections for a real frequency or as amplitude-preserving reflections for a complex frequency [10]. The second mechanism for appropriate  $\omega_R$  (such that not only the amplitude but also the phase is preserved after a cycle of reflections; in this case the process is “looped”) represents a growing eigenmode.

**6.3. Gas velocity vector is parallel to one of the sides of the plate.** Below, we restrict the analysis to a particular case when the flow is directed along the  $x$ -axis, i.e., is perpendicular to the front edge, the plate is simply supported, and there is no tension (the general case was considered in [23, 26]). In this case,  $\Delta(k_1) = \Delta(k_2)$  and  $\Delta(k_3) = \Delta(k_4)$  in view of symmetry. Then the growth condition (6.5) for the wave amplitude over a cycle of reflections reduces to the condition

$$\operatorname{Im} \Delta(k_1) < -\operatorname{Im} \Delta(k_3), \tag{6.7}$$

which expresses the following fact: the amplification of waves 1 and 2 traveling in the direction of the gas flow should be greater than the damping of waves 3 and 4 traveling against the flow. Note that since the trajectories for the chosen oscillation mode differ from each other only by the initial point while their propagation directions coincide, the amplitude variation after a cycle of reflections and condition (6.7) do not depend on a trajectory but are determined only by the oscillation mode.

Calculating  $\Delta(k_j)$  from (6.3) and solving inequality (6.7), we obtain asymptotic boundaries of single-mode flutter for each mode that are analogous to the two-dimensional boundaries (4.6):  $M^*(L_x, L_y) < M < M^{**}(L_x, L_y)$ , where

$$M^*(L_x, L_y) = \sqrt{1 + \left(\frac{n}{m}\right)^2 \left(\frac{L_x}{L_y}\right)^2} (1 + \sqrt{Dk_0^2}),$$

$$M^{**}(L_x, L_y) = \sqrt{1 + \left(\frac{n}{m}\right)^2 \left(\frac{L_x}{L_y}\right)^2} \sqrt{1 + Dk_0^2 + \sqrt{4Dk_0^2 + 1}},$$
(6.8)

$m$  and  $n$  are the half-wavelengths of the eigenmode in the directions of the  $x$ - and  $y$ -axes, and

$$k_0 = \sqrt{\left(\frac{m\pi}{L_x}\right)^2 + \left(\frac{n\pi}{L_y}\right)^2}.$$

Note that a decrease in  $L_y$  for a fixed  $L_x$  leads to an increase in the angles  $\alpha_j$  between the waves and the flow and, accordingly, to an increase in the Mach numbers for which amplification occurs.

### 7. RESULTS OF CALCULATIONS AND COMPARISON WITH ASYMPTOTIC RESULTS

Solving problem (2.6), (2.8) numerically for the four eigenfrequencies  $\omega_j^1$  ( $j = 1, \dots, 4$ ), we calculated the boundaries of the instability region in the plane  $(L_x, M)$ , i.e., the level lines  $\text{Im } \omega_j^1 = 0$ . All the calculations were performed for the problem parameters (4.3). The calculations were carried out for two configurations of plates: a series of plates (see Fig. 1b) [31] and an isolated plate (see Fig. 1c). The difference between these configurations manifests itself only in aerodynamics. In the case of a series, each plate experiences the effect of the neighboring plates whose domains of influence contain this plate. In the case of an isolated plate, the pressure distribution is different, because there are no surrounding plates.

Consider Fig. 17, which demonstrates the boundaries of the instability region in the first mode (frequency  $\omega_1^1$ ) for  $L_y = 1000, 500, 450, 400, 350$ . The solid lines show the results of calculation for a series of plates, and the dashed lines, for an isolated plate. The maximum value of length  $L_{x,\text{max}}$  for

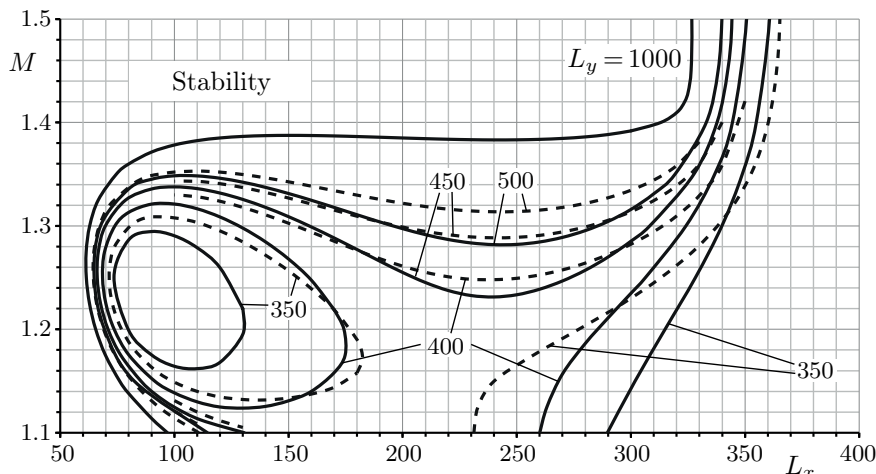


**Fig. 17.** Stability boundaries for the mode (1,1) (frequency  $\omega_1^1$ ) in the plane  $(L_x, M)$  for various values of  $L_y$  and  $1.1 < M < 1.5$ . Solid lines refer to the case of a series of plates, and dashed lines, to the case of an isolated plate.

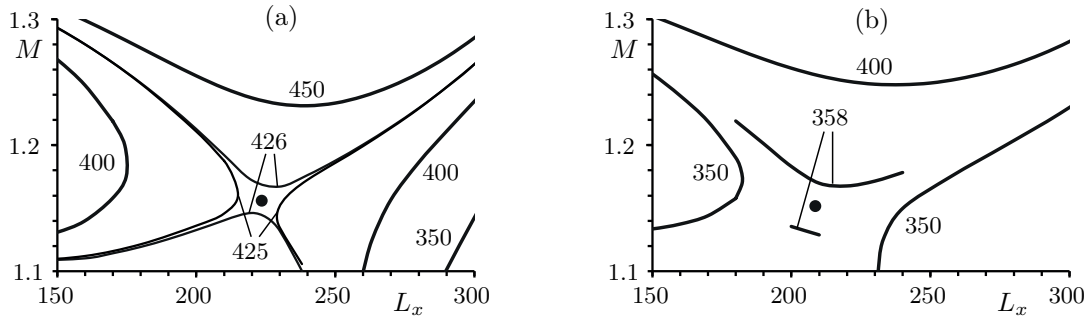


**Fig. 18.** Stability boundaries for the mode (1,1) in the plane  $(L_x, M)$  near the splitting of the boundary: (a) a series of plates and (b) an isolated plate. The saddle point is shown by a circle.

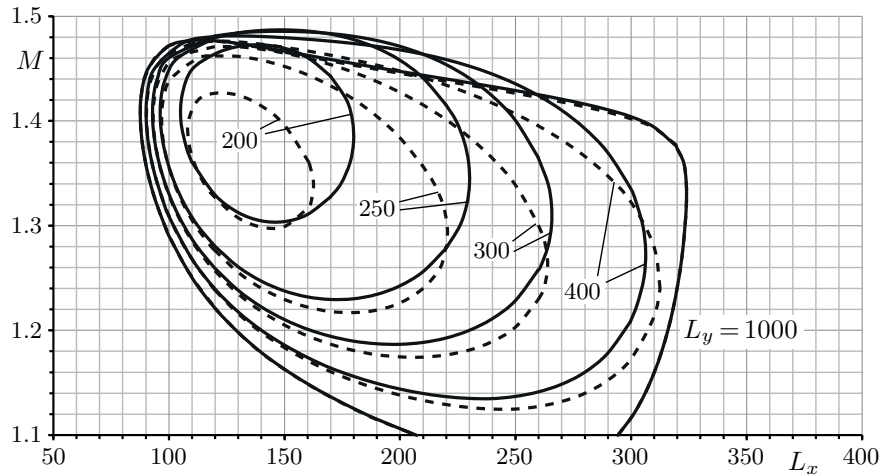


**Fig. 19.** Stability boundaries for the mode (1,2) (frequency  $\omega_2^1$ ) in the plane  $(L_x, M)$  for various  $L_y$ . Solid lines refer to the case of a series of plates, and dashed lines, to the case of an isolated plate.

which the plate is stable for any width  $L_y$  is 57 and corresponds to  $L_y = \infty$ . For  $L_x > L_{x,max}$  and sufficiently large values of  $L_y$ , there exists an interval  $M^*(L_x, L_y) < M < M^{**}(L_x, L_y)$  in which the plate is unstable in the first mode. Note that the stability boundaries for  $L_y = 1000$  almost coincide in the two cases both with each other and with the boundary calculated in the two-dimensional statement, i.e., for  $L_y = \infty$  (see Fig. 8). As the width  $L_y$  decreases, the range of Mach numbers in which the plate is unstable decreases, and for  $L_y = L_{y,s}$  the instability region is split into two isolated subregions: one, lying in the domain of smaller values of  $L_x$ , corresponds to single-mode flutter, and the other corresponds to flutter of coupled type. Figure 18 demonstrates this splitting in greater detail: a saddle point in the instability region is clearly seen at  $L_{y,s} \approx 425$  for a series and at  $L_{y,s} \approx 356$  for an isolated plate. As  $L_y$  decreases further, the domain of single-mode flutter decreases in size and contracts to a certain point. For a certain width  $L_y$ , it completely shrinks to this point and vanishes. The boundary of coupled flutter decreases much slower and shifts toward higher values of  $L_x$  as  $L_y$  decreases.

Let us proceed to analyze the stability boundaries for higher order modes. Figure 19 shows the region of flutter in the second mode (frequency  $\omega_2^1$ ) for  $L_y = 1000, 400, 300, 250, 200$ . These regions are bounded on the right by the values of  $L_x$  for which flutter of coupled type arises, because the first and second modes are “coupled” in this flutter; the first mode becomes a growing one, and the second, a damped one. Just as for the first mode, a decrease in  $L_y$  leads to a contraction of the region of single-mode flutter; for a certain  $L_y$ , this region shrinks to a point and vanishes.

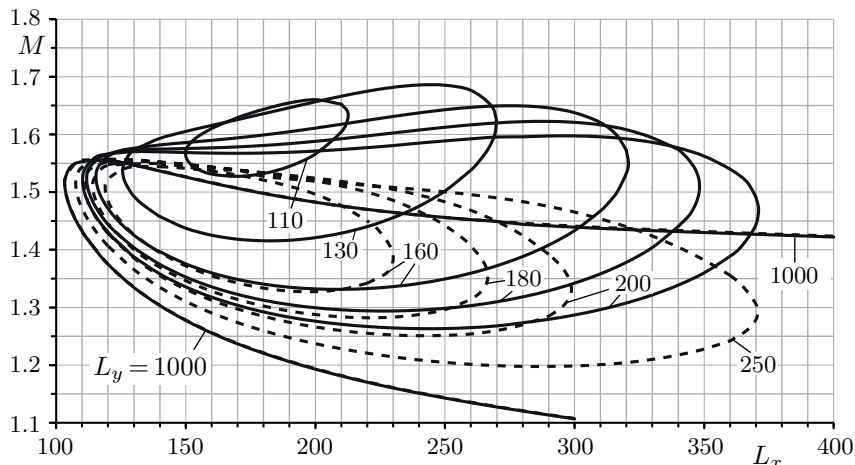


**Fig. 20.** Stability boundaries for the mode (1,3) (frequency  $\omega_3^1$ ) in the plane  $(L_x, M)$  for various values of  $L_y$ . Solid lines refer to the case of a series of plates, and dashed lines, to the case of an isolated plate.

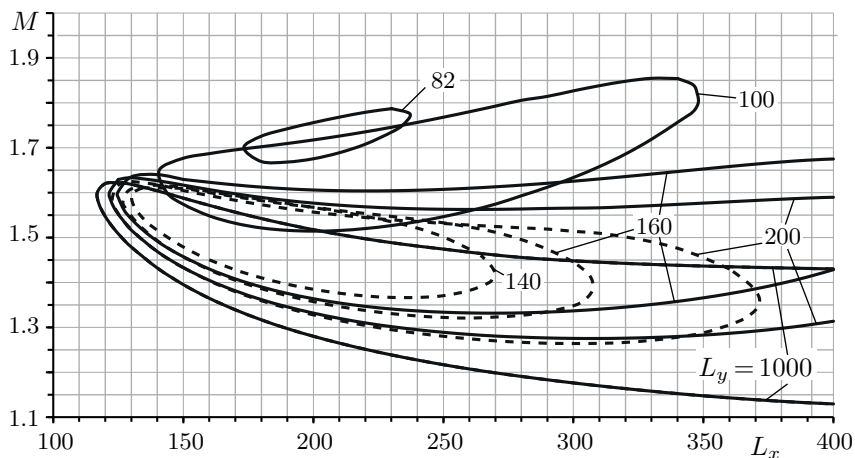


**Fig. 21.** Stability boundaries for the mode (1,4) (frequency  $\omega_4^1$ ) in the plane  $(L_x, M)$  for various values of  $L_y$ . Solid lines refer to the case of a series of plates, and dashed lines, to the case of an isolated plate.

The boundaries of the flutter region in modes 3 and 4, which do not take part in the formation of flutter of coupled type, are shown in Figs. 20 and 21, respectively. In contrast to the first two modes, for  $L_y = \infty$  they have the asymptotes  $M^* = 1$  and  $M^{**} = \sqrt{2}$  as  $L_x \rightarrow \infty$  (Subsection 5.1). The boundaries for  $L_y = 1000$  almost coincide with the results of calculation for the two-dimensional problem. As  $L_y$  decreases, the flutter regions for a series of plates move to higher values of  $M$  and become bounded on the  $L_x$ -axis. Next, just as in the case of single-mode flutter with respect to the first two modes, the instability boundaries shrink to a point and vanish.

The case of an isolated plate differs qualitatively by the fact that, as  $L_y$  decreases, the flutter regions are “embedded” in each other so that the Mach numbers corresponding to instability do not increase (see Figs. 20 and 21).

The shift of the regions of single-mode flutter of a series of plates toward higher Mach numbers with decreasing  $L_y$  is explained by the asymptotic theory of single-mode flutter. In Fig. 22, the boundaries found numerically (heavy lines) are compared with those found by the asymptotic formulas (6.8) (thin lines). Figure 22a shows the boundaries of flutter in mode 3 for  $L_y = 1000, 200, 130, 110$  (solid, dashed, dot-and-dash, and dotted lines, respectively). In Fig. 22b,

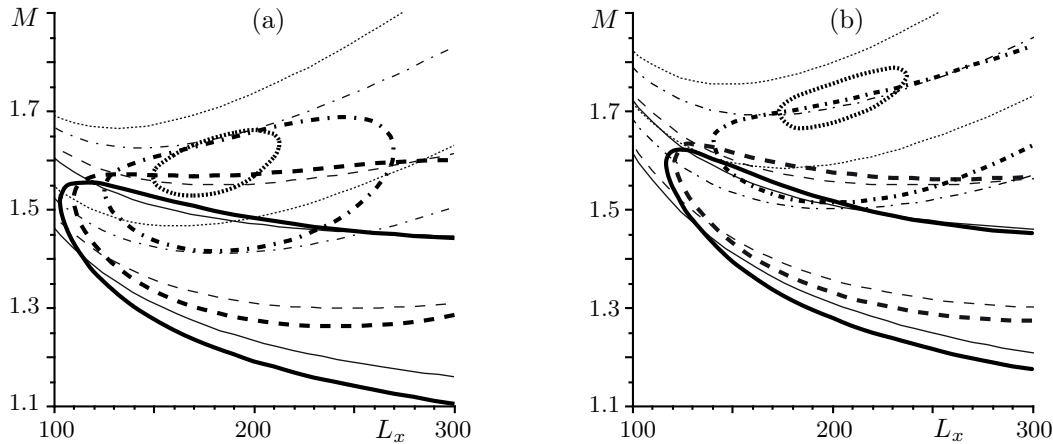


**Fig. 22.** Comparison of the boundaries of flutter obtained numerically (heavy lines) and by the asymptotic formulas (6.8) (thin lines) for modes (a) 3 and (b) 4.

similar lines show the boundaries of flutter in mode 4 for  $L_y = 1000, 200, 100, 82$ . One can see that an increase in the Mach numbers for which instability is observed is correctly described by the asymptotics in the “central” part of the flutter region  $100 \leq L_x \leq 300$ . The difference is only in the domain of small  $L_x$ , where the condition of large dimensions in the  $x$ -direction is not satisfied, and in the domain of large  $M$ , which is attained only for sufficiently small  $L_y$ , when the condition of large dimensions of the plate in the  $y$ -direction is violated. From the asymptotic point of view, the growth of  $M$  corresponding to instability is attributed to the fact that, as  $L_y$  decreases, the angle  $\alpha_j$  between the waves constituting the eigenmode and the flow increases, which leads to an increase in the Mach numbers (6.8).

For isolated plates, the absence of a similar shift is not explained by the asymptotic theory, which rapidly loses accuracy as  $L_y$  decreases. In the case of a series of plates, the perturbation of the flow by eigenmodes in a direction transverse to the flow can be represented as a superposition of two waves traveling in opposite directions along a periodically supported strip; therefore, the perturbation is correctly determined by the asymptotic theory. The only effect of the three-dimensional character of the flow is that the plane into which the plate is built in is not deformed in front of the plate. In the case of an isolated plate, the nondeformability around the lateral sides of the plate is also important, but it is not taken into account by the asymptotic theory.

## CONCLUSIONS

In this paper, we have compared the calculation results for the boundaries of single-mode and coupled flutter of an elastic plate in a supersonic flow that were obtained by the asymptotic method of global instability and by the numerical solution of the full integro-differential eigenvalue problem. We have shown that for the two-dimensional problem (a plate in the form of a strip), the boundaries of single-mode flutter are quantitatively correctly determined by the asymptotic method for a plate length  $L_x$  of about 100 or greater, which corresponds to the structures used in engineering. The asymptotic boundary of coupled flutter provides a sufficient condition for the absence of this type of flutter in plates of any length.

In the case of a series of rectangular plates linked to each other, the accuracy of the asymptotic theory decreases as the width  $L_y$  of the plates decreases; however, the theory makes a correct prediction of the increase in the Mach numbers corresponding to single-mode flutter.

In the case of an isolated plate, there is a qualitative discrepancy between the asymptotic theory and numerical calculations, because here the three-dimensional character of the perturbed gas flow over the plate, which is not taken into account in the asymptotic theory, becomes dominant.

## ACKNOWLEDGMENTS

This work is supported by the Russian Science Foundation under grant 14-50-00005.

## REFERENCES

1. L. B. Aizin and V. P. Maksimov, “On the stability of flow of weakly compressible gas in a pipe of model roughness,” *Prikl. Mat. Mekh.* **42** (4), 650–655 (1978) [*J. Appl. Math. Mech.* **42**, 691–697 (1978)].
2. V. V. Bolotin, “Dynamical edge effect under elastic vibrations of plates,” *Inzh. Sb.* **31**, 3–14 (1961).
3. O. Doaré and E. de Langre, “Local and global instability of fluid-conveying pipes on elastic foundations,” *J. Fluids Struct.* **16** (1), 1–14 (2002).
4. O. Doaré and E. de Langre, “The role of boundary conditions in the instability of one-dimensional systems,” *Eur. J. Mech. B/Fluids* **25** (6), 948–959 (2006).
5. B. Echebarria, V. Hakim, and H. Henry, “Nonequilibrium ribbon model of twisted scroll waves,” *Phys. Rev. Lett.* **96** (9), 098301 (2006).
6. Ia. A. Kameniarzh, “On some properties of equations of a model of coupled termoplasticity,” *Prikl. Mat. Mekh.* **36** (6), 1100–1107 (1972) [*J. Appl. Math. Mech.* **36**, 1031–1038 (1972)].
7. A. G. Kulikovskii, “On the stability of homogeneous states,” *Prikl. Mat. Mekh.* **30** (1), 148–153 (1966) [*J. Appl. Math. Mech.* **30**, 180–187 (1966)].
8. A. G. Kulikovskii, “On the stability of Poiseuille flow and certain other plane-parallel flows in a flat pipe of large but finite length for large Reynolds’ numbers,” *Prikl. Mat. Mekh.* **30** (5), 822–835 (1966) [*J. Appl. Math. Mech.* **30**, 975–989 (1966)].
9. A. G. Kulikovskii, “Stability of flows of a weakly compressible fluid in a plane pipe of large, but finite length,” *Prikl. Mat. Mekh.* **32** (1), 112–114 (1968) [*J. Appl. Math. Mech.* **32**, 100–102 (1968)].
10. A. G. Kulikovskii, “The global instability of uniform flows in non-one-dimensional regions,” *Prikl. Mat. Mekh.* **70** (2), 257–263 (2006) [*J. Appl. Math. Mech.* **70**, 229–234 (2006)].
11. A. G. Kulikovskii and I. S. Shikina, “On bending vibrations of a long tube with moving fluid,” *Izv. Akad. Nauk Arm. SSR, Mekh.* **41** (1), 31–39 (1988).
12. E. M. Lifshitz and L. P. Pitaevskii, *Physical Kinetics* (Nauka, Moscow, 1979; Pergamon, Oxford, 1981), Course of Theoretical Physics **10**.
13. J. W. Miles, *The Potential Theory of Unsteady Supersonic Flow* (Univ. Press, Cambridge, 1959).
14. J. W. Nichols, J.-M. Chomaz, and P. J. Schmid, “Twisted absolute instability in lifted flames,” *Phys. Fluids* **21** (1), 015110 (2009).
15. N. Peake, “On the unsteady motion of a long fluid-loaded elastic plate with mean flow,” *J. Fluid Mech.* **507**, 335–366 (2004).
16. J. Priede and G. Gerbeth, “Convective, absolute, and global instabilities of thermocapillary–buoyancy convection in extended layers,” *Phys. Rev. E* **56** (4), 4187–4199 (1997).
17. J. Priede and G. Gerbeth, “Absolute versus convective helical magnetorotational instability in a Taylor–Couette flow,” *Phys. Rev. E* **79** (4), 046310 (2009).
18. A. Shishaeva, V. Vedenev, and A. Aksenov, “Nonlinear single-mode and multi-mode panel flutter oscillations at low supersonic speeds,” *J. Fluids Struct.* **56**, 205–223 (2015).
19. G. A. Shugai and P. A. Yakubenko, “Convective and absolute instability of a liquid jet in a longitudinal magnetic field,” *Phys. Fluids* **9** (7), 1928–1932 (1997).
20. F. Tuerke, D. Sciamarella, L. R. Pastur, F. Lusseyran, and G. Artana, “Frequency-selection mechanism in incompressible open-cavity flows via reflected instability waves,” *Phys. Rev. E* **91** (1), 013005 (2015).
21. V. V. Vedenev, “Flutter of a wide strip plate in a supersonic gas flow,” *Izv. Ross. Akad. Nauk, Mekh. Zhidk. Gaza*, No. 5, 155–169 (2005) [*Fluid Dyn.* **40**, 805–817 (2005)].
22. V. V. Vedenev, “High-frequency plate flutter,” *Izv. Ross. Akad. Nauk, Mekh. Zhidk. Gaza*, No. 2, 163–172 (2006) [*Fluid Dyn.* **41**, 313–321 (2006)].
23. V. V. Vedenev, “High-frequency flutter of a rectangular plate,” *Izv. Ross. Akad. Nauk, Mekh. Zhidk. Gaza*, No. 4, 173–181 (2006) [*Fluid Dyn.* **41**, 641–648 (2006)].
24. V. V. Vedenev, “Nonlinear high-frequency flutter of a plate,” *Izv. Ross. Akad. Nauk, Mekh. Zhidk. Gaza*, No. 5, 197–208 (2007) [*Fluid Dyn.* **42**, 858–868 (2007)].
25. V. V. Vedenev, “Numerical investigation of supersonic plate flutter using the exact aerodynamic theory,” *Izv. Ross. Akad. Nauk, Mekh. Zhidk. Gaza*, No. 2, 169–178 (2009) [*Fluid Dyn.* **44**, 314–321 (2009)].
26. V. V. Vedenev, “Study of the single-mode flutter of a rectangular plate in the case of variable amplification of the eigenmode along the plate,” *Izv. Ross. Akad. Nauk, Mekh. Zhidk. Gaza*, No. 4, 163–174 (2010) [*Fluid Dyn.* **45**, 656–666 (2010)].

27. V. V. Vedeneev, "Panel flutter at low supersonic speeds," *J. Fluids Struct.* **29**, 79–96 (2012).
28. V. V. Vedeneev, "Limit oscillatory cycles in the single mode flutter of a plate," *Prikl. Mat. Mekh.* **77** (3), 355–370 (2013) [*J. Appl. Math. Mech.* **77**, 257–267 (2013)].
29. V. V. Vedeneev, S. V. Guvernyuk, A. F. Zubkov, and M. E. Kolotnikov, "Experimental observation of single mode panel flutter in supersonic gas flow," *J. Fluids Struct.* **26** (5), 764–779 (2010).
30. V. V. Vedeneev, S. V. Guvernyuk, A. F. Zubkov, and M. E. Kolotnikov, "Experimental investigation of single-mode panel flutter in supersonic gas flow," *Izv. Ross. Akad. Nauk, Mekh. Zhidk. Gaza*, No. 2, 161–175 (2010) [*Fluid Dyn.* **45**, 312–324 (2010)].
31. V. V. Vedeneev and S. V. Shitov, "Flutter of a periodically supported elastic strip in a gas flow with a small supersonic velocity," *Izv. Ross. Akad. Nauk, Mekh. Tverd. Tela*, No. 3, 105–126 (2015) [*Mech. Solids* **50**, 318–336 (2015)].
32. P. A. Yakubenko, "Global capillary instability of an inclined jet," *J. Fluid Mech.* **346**, 181–200 (1997).

*Translated by I. Nikitin*